



Technical Report  
998

# Calculation of Satellite Drag Coefficients



E.M. Gaposchkin

18 July 1994

**Lincoln Laboratory**

MASSACHUSETTS INSTITUTE OF TECHNOLOGY

LEXINGTON, MASSACHUSETTS



Prepared for the Department of the Air Force  
under Contract F19628-90-C-0002.

Approved for public release; distribution is unlimited.

94-31038



DTIC QUALITY INSPECTED 3

94 9 28 005

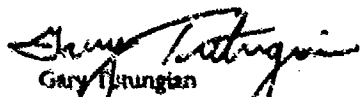
This report is based on studies performed at Lincoln Laboratory, a center for research operated by Massachusetts Institute of Technology. The work was sponsored by the Department of the Air Force under Contract F19628-90-C-0002.

This report may be reproduced to satisfy needs of U.S. Government agencies.

The ESC Public Affairs Office has reviewed this report, and it is releasable to the National Technical Information Service, where it will be available to the general public, including foreign nationals.

This technical report has been reviewed and is approved for publication.

FOR THE COMMANDER

  
Gary Thurgian  
Administrative Contracting Officer  
Contracted Support Management

Non-Lincoln Recipients

PLEASE DO NOT RETURN

Permission is given to destroy this document  
when it is no longer needed.

MASSACHUSETTS INSTITUTE OF TECHNOLOGY  
LINCOLN LABORATORY

**CALCULATION OF SATELLITE DRAG COEFFICIENTS**

*E.M. GAPOSCHKIN*  
*Group 91*

TECHNICAL REPORT 998

18 JULY 1994

Approved for public release; distribution is unlimited.

DTIC QUALITY INSPECTED 3

LEXINGTON

MASSACHUSETTS

## ABSTRACT

Calculation of  $C_d$  for satellites using accommodation coefficients is reviewed. A phenomenological model for accommodation coefficients due to Hurlbut, Sherman, and Nocilla is used to obtain values for the accommodation coefficients for average satellite materials, thermosphere constituents and temperatures, and satellite velocities using a number of laboratory measurements. There is a significant difference between these results and the traditional method of calculating  $C_d$ . These differences contribute as much as 20% error in use of thermosphere models for calculation of satellite drag.

<b>Accession For</b>	
NTIS GRA&I	<input checked="" type="checkbox"/>
DTIC TAB	<input type="checkbox"/>
Unannounced	<input type="checkbox"/>
Justification	
By _____	
Distribution/ _____	
<b>Availability Codes</b>	
<b>Dist</b>	<b>Avail and/or Special</b>
A-1	

## **ACKNOWLEDGMENT**

The author wishes to thank Professor F. Hurlbut for introducing him to the HSN theory, for several lively discussions, and for continuous encouragement.

# TABLE OF CONTENTS

Abstract	iii
Acknowledgment	v
List of Illustrations	ix
List of Tables	xi
1. INTRODUCTION	1
2. ACCOMMODATION COEFFICIENTS	3
3. DRAG COEFFICIENTS	7
4. THE HURLBUT, SHERMAN, AND NOCILLA THEORY	13
5. GOODMAN AND WACHMAN THEORY	19
6. EXPERIMENTAL DATA	21
6.1 Seidel and Steinhell	22
6.2 Musanov, Nikiforov, Omelik, and Freedlander	22
6.3 Liu, Sharma, and Knuth	23
6.4 Knuth	23
6.5 Boring and Humphris	24
6.6 Doughty and Schaezle	24
6.7 Knechtel and Pitts	25
7. DATA ANALYSIS	27
8. CALCULATION OF $C_d$	39
8.1 Comparison of Goodman and Wachman Theory and HSN Theory	39
8.2 Calculation of $C_d$ for Flat Plates	40
8.3 $C_d$ for Spheres	40
8.4 Comparison of $C_d$ with Hemero	44
9. SUMMARY	53
REFERENCES	55

## LIST OF ILLUSTRATIONS

Figure No.		Page
1	Velocity vs. kinetic energy.	1
2	Molecule number density.	2
3	Notation for surface interaction model.	5
4	Coordinate system for surface scattering calculations.	7
5	Scattering angle: helium on sapphire.	23
6	Scattering angle: aluminum.	25
7	Scattering angle: $N_2^+$ on aluminum.	25
8	Scattering angle: helium on oxygen.	36
9	Scattering velocity: helium on oxygen.	37
10	Scattering temperature: helium on oxygen.	38
11	Comparison of G&W with HSN.	39
12	Flat plate $C_d$ for $N_2$ .	40
13	Flat plate $C_d$ for helium.	41
14	$C_d$ for spherical satellites.	42
15	$C_d$ for sphere: hydrogen.	44
16	$C_d$ for sphere: helium.	45
17	$C_d$ for sphere: nitrogen.	45
18	$C_d$ for sphere: oxygen.	46
19	$C_d$ for sphere: $N_2$ .	46
20	$C_d$ for sphere: $O_2$ .	47
21	$C_d$ for sphere: argon.	47
22	$C_d$ for sphere: hydrogen.	48
23	$C_d$ for sphere: helium.	48
24	$C_d$ for sphere: nitrogen.	49
25	$C_d$ for sphere: oxygen.	49
26	$C_d$ for sphere: $N_2$ .	50
27	$C_d$ for sphere: $O_2$ .	50
28	$C_d$ for sphere: argon.	51

## LIST OF TABLES

Table No.		Page
1	Physical Constants	8
2	Atmospheric Parameters for Venus	16
3	HSN Model for Accommodation Coefficients	17
4	Data Used in Model	21
5	Grid Values for $U_{\infty}$ (km/sec)	28
6	Grid Values for $T$ , (K)	28
7	Grid Values for $\theta$ , (deg)	29
8	Grid Value $\sigma$ for $U_{\infty}$ (km/sec)	29
9	Grid Value $\sigma$ for $T$ , (K)	30
10	Grid Value $\sigma$ for $\theta$ , (deg)	30
11	Residuals for Least Squares Fit	31
12	Individual Statistics for Solution	35
13	$C_d$ for Spherical Satellites	43



## 1. INTRODUCTION

The drag force per unit mass ( $M$ ) on an element of area ( $A$ ) of a satellite is given by

$$\vec{F} = -\frac{1}{2} C_d \left( \frac{A}{M} \right) \rho V_s \vec{V}_s,$$

where  $\rho$  is the atmospheric density and  $V_s$  is the speed of the satellite with respect to the atmosphere. Analysis of satellite drag involves the product of three quantities: the projected area to mass ratio ( $A/M$ ), the ballistic coefficient ( $C_d$ ), and the atmospheric density ( $\rho$ ). None of these is known without error. General analyses [1-3] suggest that the error in calculation of drag ranges from 15% at 300- to 600-km altitudes to 30% at 800- to 1200-km altitudes. This is true, even for spherical satellites where the projected area is known without error. Due to the complexity of thermosphere models, it has been generally assumed that the error is due to inadequacies of these models. There is abundant evidence that thermosphere models have these errors [2,3]. The purpose of this discussion is to evaluate the possible error due to the uncertainty in the knowledge of  $C_d$ .

There are some limits on the focus of this report. Cook [4] provides an excellent review of the issues, which are summarized here. The mean free path  $\lambda_0$  in the thermosphere is over 200 m at an altitude of 200 km and increases to more than 600 m at 250 km. If the satellite linear dimension is  $L$ , then the Knudsen number  $K = \lambda_0/L \gg 1$  and free molecular flow occurs. Therefore, consideration is limited to calculation of  $C_d$  for free molecular flow.

In low earth orbit (LEO), the kinetic energy of molecules relative to a satellite surface is about 0.323 eV/amu or about 5 eV for atomic oxygen. LEO velocity is approximately 7.5 km/sec for circular orbits, and high eccentricity orbits can exceed this. Geosynchronous orbit (GEO) velocity is approximately 3.0 km/sec. From Figure 1 the interest in molecule kinetic energy is determined to range from 0.10 to 12 eV.

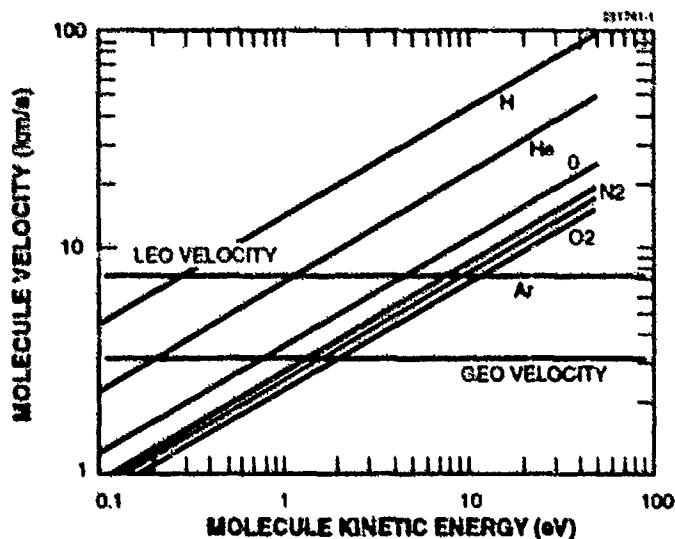


Figure 1. Velocity vs. kinetic energy.

The thermosphere constituents of concern here are H, He, N, O, N<sub>2</sub>, O<sub>2</sub>, and Ar. At 200 km, N<sub>2</sub> and O are the major constituents and have nearly the same number density. Above 600-km altitude H and He number densities are comparable with O, and N<sub>2</sub> has decreased. At higher altitudes H becomes the dominant constituent. These results are shown in Figure 2, calculated from Hedin's MSIS84 thermosphere model [4].

Finally, the numerical value of  $C_d$  is different for each constituent. Therefore, the drag force should be written

$$\vec{F} = -\frac{1}{2} \left( \frac{A}{M} \right) \left[ \sum_i C_{d_i} \rho_i \right] \vec{V}_s \vec{V}_s$$

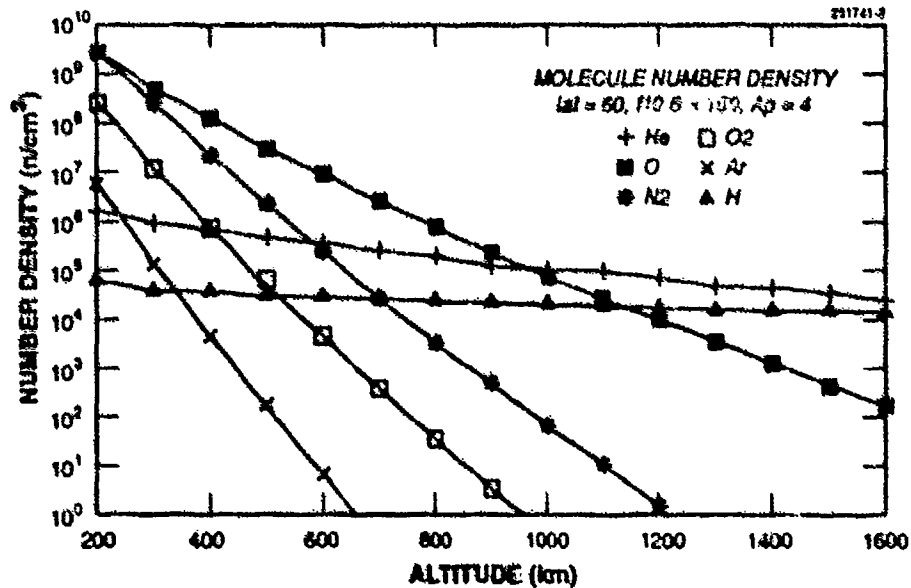


Figure 2. Molecule number density.

where  $\rho_i$  is the density for the  $i^{\text{th}}$  constituent, and  $C_{d_i}$  is the corresponding ballistic coefficient.

## 2. ACCOMMODATION COEFFICIENTS

The general theory of the interaction of a surface and a gas is not yet at the state where a physics-based model can predict the exchange of energy and momentum. Therefore, one must make use of macroscopic averages. The formulation defines three accommodation coefficients defined by the thermal accommodation coefficient

$$\alpha = \frac{E_i - E_r}{E_i - E_w},$$

the tangential momentum accommodation coefficient

$$\sigma = \frac{\tau_i - \tau_r}{\tau_i - \tau_w},$$

and the normal momentum accommodation coefficient

$$\sigma' = \frac{p_i - p_r}{p_i - p_w}.$$

$E_i$  and  $E_r$  are the energy fluxes incident on and reemitted from a surface element per unit time. The quantity  $E_w$  is the energy flux that would be carried away if all the accommodated molecules were reemitted with a Maxwellian distribution with temperature  $T_w$  (the surface temperature). So,  $\alpha$  is a measure of the amount that molecules have their energy "accommodated" to what it would be if all those reemitted had an energy  $E_w$ . For complete accommodation  $\alpha=1$ , while with no accommodation  $\alpha=0$ . Complete accommodation ( $\alpha=1$ ) is often referred to as diffuse scattering, whereas the latter ( $\alpha=0$ ) is called specular scattering.

The treatment of momentum transfer originally due to Maxwell postulated that a fraction  $(1-\sigma)$  of the incident molecules had specular scattering, and the remaining incident fraction ( $\sigma$ ) was scattered diffusely. This formulation proved to be inadequate, which led to introducing two coefficients as defined above in analogy to the expression for  $\alpha$ . In this case  $\tau$  and  $p$  are the tangential and normal momentum components. Now,  $p_w$  and  $\tau_w$  are the normal and tangential momentum components reemitted with a Maxwellian distribution  $T_w$ . Therefore,  $\tau_w=0$ . For the limiting cases of entirely specular reflection—with no energy exchange— $\alpha=\sigma=\sigma'=0$ , and for completely diffuse scattering,  $\alpha=\sigma=\sigma'=1$ .

In general, these three parameters are considered independent and will depend on properties of the gas and surface material states. In addition there is considerable evidence that these parameters vary with incident angle. Therefore, the accommodation coefficients are considered to be of the form

$$\alpha(\theta) = \frac{E_i(\theta) - E_r(\theta)}{E_i(\theta) - E_w}$$

$$\sigma(\theta) = \frac{\tau_i(\theta) - \tau_r(\theta)}{\tau_i(\theta)}$$

and

$$\sigma'(\theta) = \frac{p_i(\theta) - p_r(\theta)}{p_i(\theta) - p_w}$$

These accommodation coefficients are quite arbitrary, and a number of authors have introduced variants of the momentum coefficients that display their data to advantage. The first variant [6] defines the "relative normal momentum transfer RNT" as

$$\alpha_1 = \frac{p_i - p_r}{p_i}$$

The second variant [7,8] is to view the normal momentum coefficient as a vector quantity and define

$$\alpha_{NM} = \frac{p_i \cdot p_r}{p_i \cdot p_w}$$

The third [8,9] uses both these ideas to define

$$\alpha'_{NM} = \frac{p_i \cdot p_r}{p_i}$$

In the following, this last definition is used with the label

$$\sigma^2 = \alpha'_{NM}$$

In all cases, these coefficients are assumed to depend on the incident angle  $\theta$ .

Schamberg [10,11] introduced discussion of the scattering characteristics in addition to the amount of accommodation. He considered the angle of the (mean) reemitted beam  $\theta_r$  and the shape of the beam  $\Psi$ ; see Figure 3. Hurlbut [8,12] reviews more modern data on these properties. The issues remain. Schamberg discussed a general distribution function of scattered molecules about the mean reemitted beam. Because general models were not available at that time, he was only able to satisfactorily treat two limiting cases. He did this by introducing a mathematical relation between the  $\theta$  and  $\theta_r$ .

$$\cos\theta_r = (\cos\theta)^{\gamma}$$

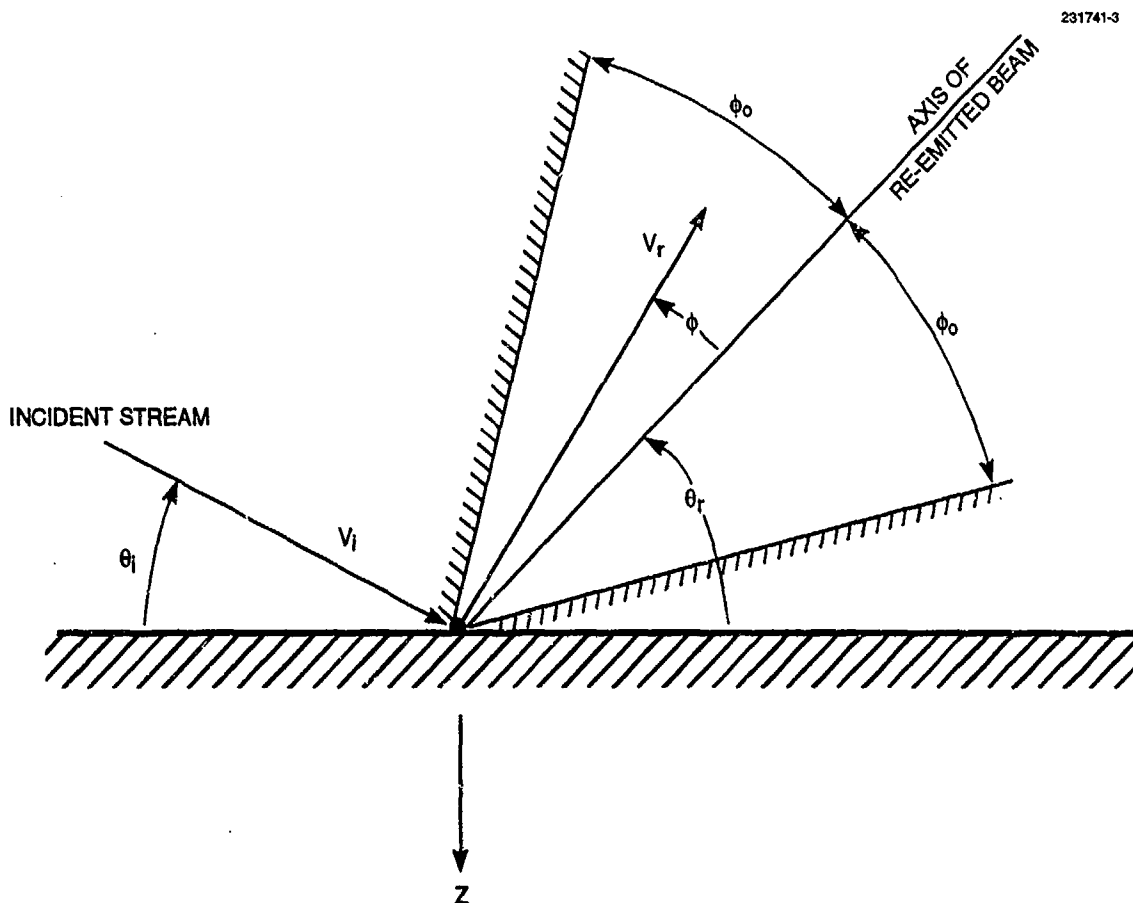


Figure 3. Notation for surface interaction model.

First is the traditional case of specular reflection for which  $\theta_r = \theta$ . This is obtained when  $\gamma = 1$ . Here, the particle reflects off the surface. Second is the case of diffuse reemission  $\gamma = \infty$ . In this case, the mean beam of reemission is at  $\theta_r = \pi/2$ , and the particles are reemitted with a Lamberian distribution. This is often characterized by saying that the particle has lost all knowledge of its incoming direction. Cook [4,13] treats these two limiting cases. The actual function  $\theta_r(\theta)$  cannot be represented by such a simple analytic function. The Hurlbut, Sherman, and Nocilla model (HSN) assumes a Maxwellian distribution for the function  $\Psi$ , while leaving  $\theta_r(\theta)$  unspecified. Part of the task of this analysis is to determine this function.

### 3. DRAG COEFFICIENTS

The modern treatment of molecular scattering of gases at a surface—leading to definition of the drag coefficient  $C_d$  and lift coefficient  $C_l$ —is presented by Schaaf [14] and Schaaf and Chambre [15]. Lacking detailed quantum mechanical models, it is customary to express the scattering in terms of the tangential momentum transfer coefficient  $\sigma$  and the normal momentum transfer coefficient  $\sigma'$ . It begins by assuming a gas in Maxwellian equilibrium, at temperature  $T$ , flowing past a surface element, with velocity  $U$ , at an angle of attack  $\theta$  (defined in Figure 4) with the distribution function

$$f = \frac{Q}{m(2\pi RT)^{\frac{3}{2}}} e^{-\frac{(\xi - U \sin\theta)^2 + (\eta + U \cos\theta)^2 + \zeta^2}{2RT}}$$

where the gas constant  $R = k/(N_A M) = 8.3145112 \times 10^7 / M$  (cm/sec)<sup>2</sup>/deg K, and  $M$  is the mass in atomic mass units (amu). Table 1 lists some basic physical constants used in the analysis.

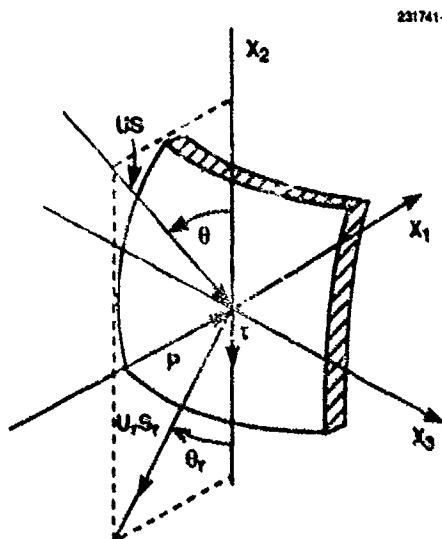


Figure 4. Coordinate system for surface scattering calculations.

**TABLE 1**  
**Physical Constants**

Boltzmann Constant	$k = 1.380658 \times 10^{-16}$	ergs/K
Avogadro's Number	$N_A = 6.0221367 \times 10^{23}$	mol <sup>-1</sup>
Stephan's Constant	$\sigma = 5.67051 \times 10^{-5}$	W cm <sup>-2</sup> K <sup>-4</sup>
	$M(p) = 1.007276470$	g/mol
	$m_p = 1.6726230 \times 10^{-24}$	grams/amu
	$1.6021773 \times 10^{-12}$	ergs/eV

Schamberg [10,11] introduced the idea of expressing the drag coefficient in terms of the thermal accommodation coefficient  $\alpha$ . Cook [4], based on Schamberg's idea, provided the treatment most often used in aeronomy studies. Alfonso et al. [16] extended Schamberg's theory to account for the Maxwellian properties of the gas.

The drag and lift from scattering off a flat surface element (Figure 4) at an incidence angle  $\theta$  can be obtained from Schaaf and Chambre [15] as

$$C_d = \sin\theta \left[ 1 - \exp(-S\theta) \right] \left\{ (2 - \sigma') \left( \sin^2\theta + \frac{1}{2S^2} \right) + \sigma \cos^2\theta + \frac{\sigma'}{2} \sqrt{\frac{\pi T_w}{T}} \frac{\sin\theta}{S} \right. \\ \left. + e^{-(S\theta)^2} \left[ \frac{2 - \sigma'}{\sqrt{\pi} S} \sin^2\theta + \frac{\sigma \cos^2\theta}{\sqrt{\pi} S} + \frac{\sigma'}{2S^2} \sqrt{\frac{T_w}{T}} \sin\theta \right] \right\}$$

and

$$C_l = \cos\theta \left[ 1 + \operatorname{erf}(S\theta) \right] \left[ (2 - \sigma') \left( \sin^2\theta + \frac{1}{2S^2} \right) + \sigma \cos^2\theta + \frac{\sigma'}{2} \sqrt{\frac{\pi T_w}{T}} \frac{\sin\theta}{S} \right] \\ + \sin\theta \cos\theta e^{-(S\theta)^2} \left[ \frac{2 - \sigma'}{\sqrt{\pi} S} + \frac{\sigma}{\sqrt{\pi} S} + \frac{\sigma'}{2S^2 \sin\theta} \sqrt{\frac{T_w}{T}} \right]$$

which depend on  $\sigma$  and  $\sigma'$ , the speed ratio  $S = U/\sqrt{2RT}$ , and, following Hurlbut [17],  $S\theta = S \sin(\theta)$ . Note that

$V_{\text{most probable}} = \sqrt{2RT}$ , used here, is the most probable velocity,  $V_{\text{av}} = \sqrt{8RT/\pi}$ , used by Alfonso et al., below, is the average velocity, and

$V_{\text{ave energy}} = \sqrt{3RT}$  is the velocity corresponding to the average thermal energy [18].

Schamberg [10,11] introduced the idea that  $C_d$  could be calculated from energy considerations and proposed

$$C_d = \left( 1 + \frac{2}{3} \sqrt{1 - \alpha} \sin\theta \right) \sin\theta$$

with the corresponding lift coefficient

$$C_l = \frac{4}{3} \sqrt{1 - \alpha} \sin\theta \cos\theta$$

Schamberg's formulation assumes the conditions  $S \gg 1$  and  $T_w \ll T$ . Schamberg discusses a general scattering pattern and adopts a Lambertian reemission model leading to these relations. However, this formulation also assumes a relation between  $\alpha$  and  $\sigma$  and  $\sigma'$ . Such a relation, if indeed it exists, will be more complex than implied by these relations.

The formulas for  $C_d$  for a sphere follow, using



$$C_d^{Sph} = \frac{1}{A} \int_{-\frac{\pi}{2}}^{\frac{\pi}{2}} \int_0^{2\pi} a^2 C_d \cos\theta \, d\lambda \, d\theta$$

where  $a$  is the radius of the sphere,  $A = \pi a^2$ , and  $C_1^{Sph} = 0$ . In this case the integral in  $\theta$  runs from  $-\pi/2$  to  $\pi/2$  to include the interaction of thermal motion on the down stream side of the sphere. The expression, assuming  $\sigma$  and  $\sigma'$  are constant, is

$$C_d^{Sph} = \left[ (2 - \sigma' + \sigma) \left( \left( 1 + \frac{1}{S^2} - \frac{1}{4S^4} \right) \text{erf}(S) + \left( 1 + \frac{1}{2S^2} \right) \frac{e^{-S^2}}{\sqrt{\pi}S} \right) + \frac{2}{3} \frac{\sigma'}{S} \sqrt{\frac{\pi T_w}{T}} \right]$$

Using Schamberg's formulation, we have

$$C_d^{Sph} = \frac{1}{A} \int_0^{\frac{\pi}{2}} \int_0^{2\pi} a^2 \left[ 1 + \frac{2}{3} \sqrt{1-\alpha} \sin\theta \right] \sin\theta \cos\theta \, d\lambda \, d\theta = 2 \left[ 1 + \frac{4}{9} \sqrt{1-\alpha} \right]$$

Here, the integral in  $\theta$  runs from 0 to  $\pi/2$ . They do reduce to the same result for the limiting case where  $S \gg 1$ ,  $T_w \ll T$  and  $\alpha = \sigma = \sigma' = 1$ .

Now Alfonso et al., tried to include the effects of the Maxwell gas average thermal velocity,  $V_t = \sqrt{(8RT/\pi)}$ , in Schamberg's formulation and derived

$$C_d^{Sph} = \begin{cases} \left( 1 + \frac{4}{9} \sqrt{1-\alpha} \right) \left[ 2 + \frac{4}{3} \left( \frac{V_t}{V_s} \right)^2 - \frac{2}{15} \left( \frac{V_t}{V_s} \right)^4 \right] & V_s > V_t \\ \left( 1 + \frac{4}{9} \sqrt{1-\alpha} \right) \left[ \frac{8}{3} \left( \frac{V_t}{V_s} \right) + \frac{8}{15} \left( \frac{V_t}{V_s} \right) \right] & V_s < V_t \end{cases}$$

In the case when  $\alpha = \sigma = \sigma' = 1$  and  $T_w \ll T$ , the Schaaf and Chambre formula reduces to the slightly different relation

$$C_d^{Sph} = 2 + \frac{\pi}{2} \left( \frac{V_t}{V_s} \right)^2 - \frac{\pi^2}{32} \left( \frac{V_t}{V_s} \right)^4$$

Using  $V_{av \text{ energy}}$  for the thermal velocity, the relation becomes

$$C_d^{Sph} = 2 + \frac{4}{3} \left( \frac{V_{av \text{ energy}}}{U} \right)^2 - \frac{2}{9} \left( \frac{V_{av \text{ energy}}}{U} \right)^4 .$$

The Schaaf and Chambre [15], Schamberg [10,11], and Alfonso et al. [16] formulations cannot be reconciled. We adopt the Schaaf and Chambre formulation.

#### 4. THE HURLBUT, SHERMAN, AND NOCILLA THEORY

In a number of discussions of rare gas solid interactions for satellite regimes (i.e., with satellite velocities and thermosphere composition), Hurlbut [8,12] has summarized the existing data on satellite accommodation coefficients. Nocilla pointed out the characteristic of the scattered gas being a "drifting Maxwellian," and Hurlbut and Sherman [19] developed a formalism for mathematically describing this process, called the Hurlbut, Sherman, and Nocilla (HSN) theory. In this section, the results are given, without approximation, in the form used for the subsequent analysis.

The HSN theory postulates an incident Maxwell gas with velocity  $U$ , temperature  $T$ , impinging a surface at an angle  $\theta$ . The particles are scattered with a velocity  $U_r$  and temperature  $T_r$  at an angle  $\theta_r$ . Given these six variables, the molecular weight, isentropic exponent  $\gamma$ , and the temperature of the scattering surface  $T_w$ , the HSN theory predicts  $\alpha$ ,  $\sigma$ , and  $\sigma'$ . Recall that the adiabatic exponent  $\gamma = 5/3$  for point atoms,  $\gamma = 7/5$  for diatomic atoms, and  $\gamma = 4/3$  for polyatomic atoms [18]. The elements of the theory, as described in Hurlbut [17], are as follows.

Following Schaaf, Hurlbut [17] finds the normal momentum flux  $p_r$  of a particle scattered from a surface

$$p_r = \frac{\rho U^2}{2\sqrt{\pi}S^2} \left[ (1-\sigma') \left( (S\theta) e^{-(S\theta)^2} + \sqrt{\pi} \left( \frac{1}{2} + (S\theta)^2 \right) (1 + \text{erf}(S\theta)) \right) + \frac{\sigma'}{2} \sqrt{\frac{\pi T_w}{T}} (e^{-(S\theta)^2} + \sqrt{\pi} (S\theta) (1 + \text{erf}(S\theta))) \right]$$

This leads to the expression for  $\sigma'$  as

$$\sigma' = \frac{\chi^*(S\theta) - \sqrt{\frac{T_r}{T}} \frac{\chi(S\theta)}{\chi(S, \theta_r)} \chi^*(S, \theta_r)}{\chi^*(S\theta) - \frac{1}{2} \sqrt{\frac{\pi T_w}{T}} \chi(S\theta)}$$

where

$$\chi(S\theta) = e^{-(S\theta)^2} + \sqrt{\pi} (S\theta) (1 + \text{erf}(S\theta))$$

and

$$\chi^*(S\theta) = (S\theta) \chi(S\theta) + \frac{\sqrt{\pi}}{2} (1 + \text{erf}(S\theta))$$

Now the net tangential momentum  $\sigma$  imparted to scattered molecules leads to

$$\sigma = 1 - \frac{S U_r^2}{U^2 S_r} \sqrt{\frac{T_r}{T}} \frac{\cos(\theta_r)}{\cos(\theta)}$$

or

$$\sigma = 1 - \frac{U_r \cos(\theta_r)}{U \cos(\theta)}$$

which is somewhat more intuitive.

The equation for  $\alpha$  can be obtained from Hurlbut and Sherman [19] as

$$\alpha = \frac{T \left[ \Psi(S, \theta) + \frac{5-3\gamma}{2(\gamma-1)} \chi(S\theta) \right] - T_r \left[ \frac{\Psi(S_r, \theta_r) \chi(S\theta)}{\chi(S_r, \theta_r)} + \frac{5-3\gamma}{2(\gamma-1)} \chi(S\theta) \right]}{T \left[ \Psi(S, \theta) + \frac{5-3\gamma}{2(\gamma-1)} \chi(S\theta) \right] - \frac{\gamma+1}{2(\gamma-1)} T_w \chi(S\theta)}$$

where

$$\Psi(S, \theta) = (S^2 + 2) e^{-\frac{(S\theta)^2}{2}} + \sqrt{\pi} \left( S^2 + \frac{5}{2} \right) (S\theta) (1 + \operatorname{erf}(S\theta))$$

which for  $S \gg 1$  reduces to  $\Psi(S, \theta) \approx 2\sqrt{\pi} S^2 (S\theta)$ . Then  $\alpha$  is approximately

$$\alpha \approx \frac{T \left[ S^2 + \frac{5-3\gamma}{2(\gamma-1)} \right] - T_r \left[ \frac{\Psi(S_r, \theta_r)}{\chi(S_r, \theta_r)} - \frac{5-3\gamma}{2(\gamma-1)} \right]}{T \left[ S^2 + \frac{5-3\gamma}{2(\gamma-1)} \right] - T_w \frac{\gamma+1}{2(\gamma-1)}}$$

A useful result obtained when  $S\theta \gg 1$  and  $T_w \ll T$  is

$$\tan(\theta_r) = \left( \frac{1-\sigma'}{1-\sigma} \right) \tan(\theta)$$

The resulting equations provide a self-consistent computation for the three accommodation coefficients  $\alpha$ ,  $\sigma$ , and  $\sigma'$  in terms of  $U$ ,  $T$ ,  $\theta$ ,  $U_r$ ,  $T_r$ ,  $\theta_r$ ,  $T_w$ , and  $\gamma$ . These values of the reflected parameters  $U_r$ ,  $T_r$ , and  $\theta_r$  must be determined from measurements. Assume that there are observations of  $\alpha(\theta)$ ,  $\sigma(\theta)$ , and  $\sigma'(\theta)$  for a given  $T$ ,  $U$ ,  $\gamma$ , and  $T_w$ . We can proceed as follows.

Consider the three simultaneous equations

$$\begin{bmatrix} \sigma \\ \sigma' \\ \alpha \end{bmatrix} = \begin{bmatrix} \sigma(U_r, \theta_r) \\ \sigma'(U_r, T_r, \theta_r) \\ \alpha(U_r, T_r, \theta_r) \end{bmatrix}$$

where  $U$ ,  $T$ ,  $\theta$ ,  $T_w$ , and  $\gamma$  are known constants. Given the three quantities  $\sigma$ ,  $\sigma'$ , and  $\alpha$ , the values of  $U_r$ ,  $T_r$ , and  $\theta_r$  are not independent but must be determined as a set. A numerical inversion of these equations can be obtained without making the  $S \gg 1$  and  $S_r \gg 1$  approximation. An important side result is that because  $U_r$  and  $T_r$  must both be positive quantities, not all combinations of  $\sigma$ ,  $\sigma'$ , and  $\alpha$  are possible.

Start by using the equation for  $\sigma$  to obtain  $U_r$  as a function of  $\theta_r$  and  $\sigma$ ,  $U_r = U(1-\sigma) \frac{\cos \theta}{\cos \theta_r}$ .

Then, use this value in the equation for  $\sigma'$  to obtain  $T_r$ . This is done by iteration. With a little algebra one can obtain the following equation, which converges rapidly by iteration.

$$T_r = \sqrt{\frac{T}{2R}} \left( \frac{\chi^*(S\theta) - \sigma' \left( \chi^*(S\theta) - \frac{\sqrt{\pi}}{2} \sqrt{\frac{T_w}{T}} \chi(S\theta) \right)}{\chi(S\theta)} - \frac{U_r \sin \theta_r}{\sqrt{2RT}} \right) 2U_r \sin \theta_r (1+x)$$

where

$$x = \frac{e^{-(S\theta_r)^2}}{\sqrt{\pi}(S\theta_r)(1+\text{erf}(S\theta_r))}$$

$$\chi(S\theta) = e^{-(S\theta)^2} + \sqrt{\pi}(S\theta)(1+\text{erf}(S\theta))$$

and

$$\chi^*(S\theta) = (S\theta)\chi(S\theta) + \frac{\sqrt{\pi}}{2}(1+\text{erf}(S\theta))$$

where  $x$  contains the only dependence on  $T_r$ . In effect we have the function  $T_r(\theta_r)$  without any approximation. One can now compute  $\alpha(U_r(\theta_r), T_r(\theta_r), \theta_r)$ , and numerically find the value of  $\theta_r$  that corresponds to the given value of  $\alpha$ . In doing this calculation for the full range of  $\theta_r$ , it is immediately apparent that a limited range of  $\alpha$  is obtained for a given pair of  $\sigma$  and  $\sigma'$ .

As an illustration, we take the example from Hurlbut [17] for a proposed Magellan Aeropass of Venus. Table 2 provides the atmospheric parameters for Venus at 140-km altitude.

Hurlbut was illustrating the relation between the accommodation coefficients  $(\alpha, \sigma, \sigma')$  and the scattered parameters  $(U_r, T_r, \theta_r)$ . His results were based on approximations, where this computation is done without approximation. The computation begins by choosing the values for  $\alpha$ ,  $\sigma$ , and  $\sigma'$  given in the first three columns. The numerical inversion is performed as described above. The first two lines of the table give good inversions. Added to the table are values of the minimum and maximum values  $\alpha_{\min}$  and  $\alpha_{\max}$  and the angle corresponding to the latter  $\theta_{r(\max)}$ . For the other cases chosen by Hurlbut, rows 3 through 8, the value of  $\alpha$  falls outside the allowable range. Four additional lines to the table were added, choosing a value of  $\alpha$  within the allowable range, and the inversion is successful.

**TABLE 2**  
**Atmospheric**  
**Parameters for**  
**Venus**

$T_w = 393 \text{ K}$
$T = 225 \text{ K}$
$S = 23.27$
$U = 7.85 \text{ km/sec}$
$R = 253$
$\gamma = 1.42$
Mol.wt. = 32.86
$\theta = 30 \text{ deg}$
Altitude = 140 km

This analysis leads to a question. The range of  $\alpha$  could be restricted further by assuming that  $T > T_w$ . Intuitively, it would seem plausible that an accommodated molecule would always scatter with a temperature greater than the scattering surface. However, this seems to impose some physics from what is fundamentally a phenomenological model. In addition intuitively one might believe that  $\theta_s > \theta$ . This is borne out by the data on neutral molecules but, as will be shown in Table 3, not for ions.

**TABLE 3**  
**HSN Model for Accommodation Coefficients**

$\sigma$	$\sigma'$	$\alpha$	$\theta_r$	$U_r$	$T_r$	$S_r$	$\alpha_{min}$	$\alpha_{max}$	$\theta_{max}$
0.60	0.60	0.80	28.9	3106	1880	3.185	0.693	0.835	33.7
0.60	0.60	0.75	17.6	2853	4780	1.835	0.693	0.835	33.7
0.90	0.90	0.90				0.539	0.968	0.993	47.8
0.90	0.90	0.80				0.381	0.968	0.993	47.8
0.80	0.80	0.90				1.298	0.906	0.959	39.1
0.80	0.80	0.80				0.830	0.906	0.959	39.1
0.90	0.85	0.90				0.630	0.951	0.988	53.7
0.90	0.85	0.95				0.870	0.951	0.988	53.7
0.85	0.90	0.90				0.790	0.959	0.983	36.3
0.85	0.90	0.95				1.118	0.959	0.983	36.3
0.90	0.90	0.97	5.6	603	1306	0.840	0.968	0.993	47.8
0.80	0.80	0.93	23.1	1478	1643	1.625	0.906	0.959	39.1
0.90	0.85	0.96	22.8	737	1580	0.825	0.951	0.988	53.7
0.85	0.90	0.96	2.4	1021	1343	1.238	0.959	0.983	36.3

## 5. GOODMAN AND WACHMAN THEORY

The Schamberg theory for calculation of ballistic coefficients uses the thermal accommodation coefficient  $\alpha$  to characterize the scattering. Many aeronomy studies use the formulation by Cook [4] for this calculation. The basic idea is as follows. From the simple classical theory, the energy exchange between two smooth, hard spheres leads to the elementary result

$$\alpha = \frac{4\mu}{(1+\mu)^2}$$

for the mass ratio  $\mu = M/M_w < 1$ , where  $M$  is the mass of the incident molecule and  $M_w$  is the mass of the surface atom. Cook [4] argues that for most satellite surfaces, the outer layer is primarily oxygen. This is either from aluminum oxide or silicates that are used for solar cells or adsorption of atomic oxygen. Therefore, we adopt  $M_w = 16$  in the following analysis. In Baule's original analysis [20], with collisions between hard spheres, for averages over all angles of incidence, the result is

$$\alpha = \frac{2\mu}{(1+\mu)^2}$$

Goodman and Wachman [21] derived a formula for  $\alpha(T)$  based on a lattice theory and experimental data. Though not directly applicable to the satellite context, it gives a working relation to be used in the context of the Schamberg formulation. Goodman and Wachman find the relation

$$\alpha(\infty) = \frac{2.4\mu}{(1+\mu)^2}$$

for the hard sphere limit with  $\mu < 0.84$ . The final result is

$$\alpha(T) = 1 - e^{-\frac{T_0}{T}} + \alpha(\infty) \tanh \left[ \frac{\sqrt{MT} a}{\alpha(\infty) \lambda} \right] e^{-\frac{T_0}{T}}$$

where  $T_0$ ,  $a$ , and  $\lambda$  are physical properties of the scattering surface. From Table II of Goodman and Wachman, we can adopt the following values for typical satellite surfaces:  $T_0 = 0$ ,  $a = 1.45 \text{ \AA}^{-1}$ , and  $\lambda = 670 \text{ (g}^{\frac{1}{2}} \text{ deg}^{\frac{1}{2}}/\text{mole}^{\frac{1}{2}} \text{ \AA)}$ . This reduces to

$$\alpha(T) = \alpha(\infty) \tanh \left[ \frac{\sqrt{MT} a}{\alpha(\infty) \lambda} \right]$$

For the range of temperature considered here, we use  $\alpha(\infty)$  in the following numerical examples for the thermal accommodation coefficient.



## 6. EXPERIMENTAL DATA

The Hurlbut, Sherman, and Nocilla (HSN) theory is based on properties of the incident flux ( $U$ ,  $T$ ,  $\theta$ ) and the reflected flux ( $U_r$ ,  $T_r$ ,  $\theta_r$ ) as well as  $M$ ,  $T_w$  and  $\gamma$ .  $U_r$ ,  $T_r$ , and  $\theta_r$  would be the underlying variables of the scattering process. We would like to have a reductionist model that predicts  $U_r$  ( $U$ ,  $T$ ,  $\theta$ ,  $T_w$ ,  $\gamma$ , gas constituents, scattering surface properties),  $T_r$  ( $U$ ,  $T$ ,  $\theta$ ,  $T_w$ ,  $\gamma$ , gas constituents, scattering surface properties), and  $\theta_r$  ( $U$ ,  $T$ ,  $\theta$ ,  $T_w$ ,  $\gamma$ , gas constituents, scattering surface properties). Today, no such model exists.

There are some experimental data and, therefore, we seek an empirical model that is limited to the satellite context as defined above. The experimental data sets are listed in Table 4.

TABLE 4  
Data Used in Model

Source		Energy (eV)	Velocity (km/sec)	$\langle \cos \theta \rangle$	$\sigma$
Seidel and Steinheil	He	0.05	1.77	-0.001	0.012
Musanov and Nikiforov	N <sub>2</sub>	2.0	4.2	0.000	0.008
Liu, Sharma, Knuth	He	1.0	6.946	-0.007	0.046
Boring and Humphris	N <sub>2</sub>	8.0	7.42	0.003	0.021
Doughty and Schaezle	Ar	25.0	10.99	0.001	0.031
Boring and Humphris	N <sub>2</sub>	25.0	13.13	-0.051	0.102
Doughty and Schaezle	N <sub>2</sub>	25.0	13.13	-0.001	0.023
Knechtel and Pitts	N <sub>2</sub> <sup>+</sup>	10.0	8.3		

These are all data of the momentum accommodation coefficients in nearly satellite conditions. There is no data of the three accommodation coefficients together. We have selected data sets with velocities

corresponding to near-earth orbits. In addition, data sets were limited to those corresponding to Cook's prescription, i.e., where a reasonable assumption that oxygen was the principal scattering atom.

These data sets have a number of limitations. First, there is no data on the thermosphere constituents: N, O, H, and O<sub>2</sub>. Second, all the results are given in graphical form. Lacking tabular data, the numerical values of  $\sigma$  and  $\sigma'$  were necessarily read from the curves with a consequent increase in error. The numerical values are given in Table 11. The standard error of fit of the model to the data is 0.026, and the mean and standard error for each data set is given in Table 12. Finally, the experimental conditions are not thoroughly known. For example, we do not know the appropriate values for the Maxwell gas temperature  $T$  (700 K was assumed), though we do know the velocity. Also, the temperature of the scattering sample  $T_s$  was not given and was assumed to be 300 K. A brief description of each data set follows.

### 6.1 SEIDEL AND STEINHEIL (1974)

The description of the experimental set up stated that the He velocity was 1770 m/sec. However, it was also stated that this corresponds to an energy of 0.05 eV. He at 1.770 km/sec has a energy of 0.065 eV, and He with an energy of 0.05 eV has a velocity of 1.553 km/sec. We have chosen to characterize the data with a velocity of 1.770 km/sec.

Seidel and Steinheil chose to give their results in terms of  $\sigma$  and the "relative normal momentum transfer RNT"  $\alpha_1'$ . For use here, it was converted to  $\sigma'' = 2 - \alpha_1'$ .

Seidel and Steinheil plotted results for He scattering off copper, shellac, tungsten, gold, glass, and sapphire. Following Cook's reasoning, we selected the sapphire data as a sapphire, Al<sub>2</sub>O<sub>3</sub>, surface is most likely to present oxygen as the scattering object.

These data are used to obtain an initial evaluation of the reflected scattering angle  $\theta_r$ . Using the approximate formula for  $\theta_r$ , we can calculate  $\theta_r$  from  $\sigma, \sigma'$ , and  $\theta$ . As seen in Figure 5, for He at 1.77 km/sec,  $\theta_r$  is a monotonically increasing function of  $\theta$ . At incident angles approaching 90 deg, it is nearly equal to  $\theta$ . This is the condition for specular reflection.

### 6.2 MUSANOV, NIKIFOROV, OMELIK, AND FREEDLENDER (1985)

These authors [22] provide data for N<sub>2</sub> scattering off of aluminum, duralium, steel, and a variety of tin surfaces. The N<sub>2</sub> velocity is given as 2 eV or 4.2 km/sec. They claim a velocity ratio of  $S = 5.5 \pm 0.7$ , which would suggest a Maxwell temperature of  $T = 982$  K. Because of the uncertainty of  $S$ , we have adopted  $T = 700$  K consistent with the other data sets. The authors also state that  $T_s = 310 \pm 20$  K. Because of the uncertainty, we have adopted  $T_s = 300$  K consistent with the other data sets.

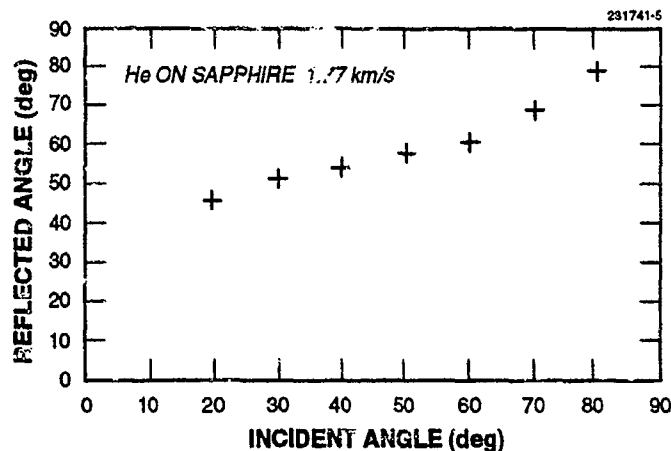


Figure 5. Scattering angle: helium on sapphire.

Musanov et al. have reduced their data and provide an analytical expression that can be used to obtain  $\sigma$  and  $\sigma'$ . We have chosen the data for aluminum, assuming that it is in fact  $\text{AlO}_2$ . The expressions are

$$\sigma = 1.01$$

and

$$\sigma' = 0.5906 - 0.1044 \cos(2\theta)$$

These expressions were evaluated between 0 and 90 deg at 10-deg intervals. These become the tabular data used in the least squares determination of model parameters.

### 6.3 LIU, SHARMA, AND KNUTH (1979)

These experiments used 1 eV (6.946 km/sec) He particles impinging on an aluminum plate and an anodized aluminum plate. They studied scattering as a function of incident angle in terms of the distribution of scattered particles in the plane containing the incident beam and the surface normal as well as the distribution out of this plane. They adopted the representation of  $\alpha_{TM} = \sigma$  and  $\alpha_{TM}$  to represent the data. The latter were converted to  $\sigma'$  using  $T_w = 300$  K.

### 6.4 KNUTH (1930)

Knuth did not publish any new measurements. However, he converted a number of existing normal momentum accommodation coefficient's measurements into the variable  $\sigma'' = \alpha_{TM}$  and published

the numerical values. The purpose was to demonstrate that a simple model could be used for this variable, i.e.,  $\sigma'' = 1 + \theta/90$ ,  $\theta$  expressed in degrees. He did provide a table of values taken from the same authors described here. With the view of examining this simple relation, this data were also included in the determination of the HSN model parameters.

## 6.5 BORING AND HUMPHRIS (1970)

This experimental data [23] was of  $N_2$  in the energy range 8–200 eV, 7–37 km/sec. The experiments were done on samples of the material used for the Echo I and Echo II satellites. Echo I was aluminum evaporated on Mylar, and Echo II was aluminum with a coating of Alodine, an amorphous phosphate. The Echo I data was chosen for this analysis. Data was read from the curves at 8 eV, 7.4 km/sec and 25 eV, 13.13 km/sec, the higher velocities being much greater than an expected satellite velocity.

Boring and Humphris provide the observable

$$\frac{P_m}{P_o} = (2 - \sigma - \sigma') \cos^2 \theta - (1 - \sigma) + 0.055 \cos \theta$$

This is used directly in the computation of the HSN model parameters.

## 6.6 DOUGHTY AND SCHAETZLE (1969)

Doughty and Schaetzle [24] made measurements of  $N_2$ , air, and Ar covering the energy range 4–200 eV. Schaetzle [25] describes the experimental setup. Their scattering materials included aluminum and fresh varnish. Only data on normal scattering,  $\theta = 90$  deg, was given covering the full energy range. The data for different incidence angles were given for 25, 75, and 150 eV. Only the 25 eV data (10.99 km/sec for Ar and 13.13 km/sec for  $N_2$ ) are used in this analysis. All of this data exhibits the characteristic  $\sigma > 1.0$  for some range of  $\theta$ . This leads to "forward scattering," i.e.,  $\theta > 90$  deg where the scattered molecule reverses direction. This is shown in Figure 6. Note the range for  $\theta$ , is 0 to 180 deg and that  $\theta_r = 112.6$  deg at  $\theta = 60$  deg for both  $N_2$  and Ar. In other words, the lobe of the reflection pattern is bent rearward rather than in the forward direction.

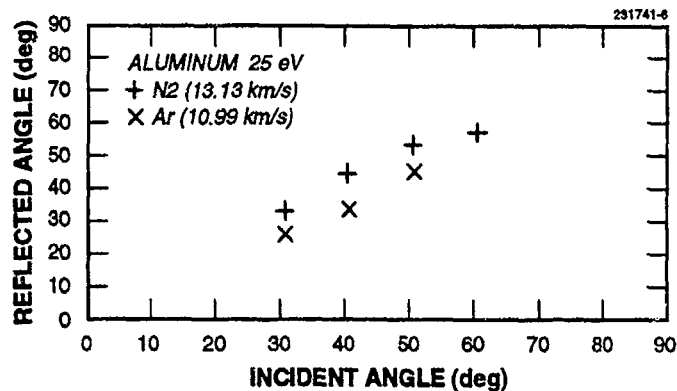


Figure 6. Scattering angle: aluminum.

## 6.7 KNECHTEL AND PITTS (1969, 1973)

The data [26,27] are taken with N<sub>2</sub><sup>+</sup> at 5, 10, 15, and 20 eV (5.87, 8.30, 10.17, and 11.74 km/sec). The scattering surface is aluminum. Figure 7 plots the reflected scattering angle  $\theta_r$ . The behavior of  $\theta_r$  is quite different than the two previous examples. We found that the ion data could not be made consistent with the other data used in this analysis, and the data were not included in the determination of the HSN model parameters.

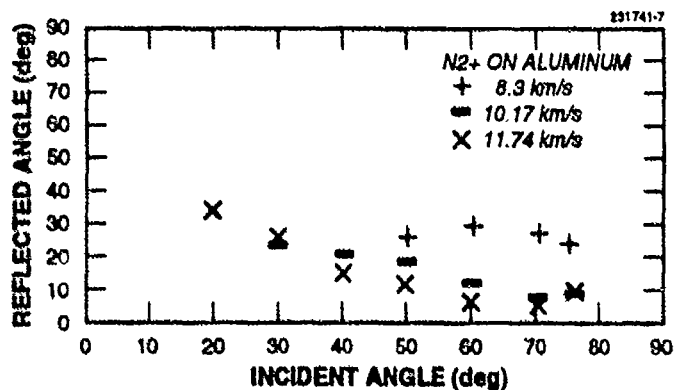


Figure 7. Scattering angle: N<sub>2</sub><sup>+</sup> on aluminum.

## 7. DATA ANALYSIS

The data analysis began by computing, where possible,  $\theta_r$  from the approximate formula. The evidenced backscattering mentioned by Hurlbut is seen. This is particularly evident in the high-velocity measurements of Doughty and Schaetzle where the scattering angle exceeds 90 deg. In general, for each data set,  $\theta_r$  increases monotonically with  $\theta$  and  $\theta_r > \theta$ . However, the data for  $N_2^+$  is anomalous in that  $\theta_r < \theta$  and monotonically decreases. The data on  $N_2^+$  were not used in the analysis. We assume that this model is inappropriate for ions.

Motivated by the Baule model for  $\alpha$ , an attempt was made to find a relation in terms of the mass ratio. In this data, the mass ranges from 4 to 40 amu. However, the large difference in mass for  $N_2$  and Ar, and the small difference in  $\sigma$  and  $\sigma'$  for the two constituents, frustrated this model dependence.

Finally, a model that depended only  $U$ ,  $\theta$ , and the mass ratio  $\mu$  was found to be acceptable. The model dependence adopted is then  $U_r = U_r(U, \theta, \mu)$ ,  $T_r = T_r(U, \theta)$ , and  $\theta_r = \theta_r(U, \theta)$ . This was done by referring all the constituents to He. The He model was implemented as follows. A grid of points  $(U, \theta_r)$  is defined separately for  $U_r$ ,  $T_r$ , and  $\theta_r$ . For a given  $U, \theta$  combination, linear interpolation is used within this grid, i.e., a ruled surface. The values of the functions ( $U_r$ ,  $T_r$ , and  $\theta_r$ ) at the grid points are determined by a least squares computation, as described below. Then, the values of  $U_r$  for the constituent  $x$  is computed from

$$U_r^x = U_r^{He} - 0.01427 \left[ \left( \frac{\mu^x}{\mu^{He}} \right)^{\frac{3}{2}} - 1 \right]$$

where  $\mu$  is computed assuming oxygen is the scattering atom. The values for  $T_r$  and  $\theta_r$  are used without correction.

The grid point values were determined with an iterative least squares program that accepts as input the grid point model and observations of  $\alpha$ ,  $\sigma$ ,  $\sigma'$ ,  $\sigma''$ , and the linear combination observed by Boring and Humphris  $(2 - \sigma - \sigma') \cos^2 \theta - (1 - \sigma) + 0.055 \cos \theta$ . This nonlinear least squares computation was iterated until convergence. It is found that, because of the large value of the speed ratio  $S = U/\sqrt{2RT}$ , the coefficients for  $U$  and  $T$  are almost completely correlated numerically. This was overcome by applying weak prior knowledge [28], using an initial variance of the temperature variable of  $\pm 1000$  K. This required choosing the initial values of  $T$ , which was done by experiment. In addition, from symmetry considerations, the values of  $\theta_r$  ( $\theta = 90$  deg) were constrained to be 90.0 deg. The final least squares solution used 105 observations, had a mean error of -0.003, and a standard error of 0.025. The total data set fit this model with an accuracy of 2.5%. Table 5 lists the grid values for  $U_r$ , Table 6 lists the grid values for  $T_r$ , and Table 7 lists the grid values for  $\theta_r$ . Tables 8, 9, and 10 give the formal standard error  $\sigma$  for each grid point.

**TABLE 5**  
Grid Values for  $U_r^{1/2}$  (km/sec)

$U(\text{km/sec}) \backslash \theta$	0.0	45.0	90.0
1.77	2.146	0.840	0.225
4.20	2.806	4.041	3.989
6.946	4.020	3.143	3.174
10.990	7.367	7.557	5.649
13.130	7.744	4.944	4.474

**TABLE 6**  
Grid Values for  $T_r$  (K)

$U(\text{km/sec}) \backslash \theta$	0.0	45.0	90.0
1.77	1	35	75
13.130	992	1003	997

**TABLE 7**  
**Grid Values for  $\theta$ , (deg)**

U(km/sec)\ $\theta$	0.0	30.0	45.0	60.0	75.0	90.0
1.770	74.3	70.1	65.8	67.1	71.4	90.0
4.200	96.5	91.2	91.3	90.8	90.4	90.0
6.946	89.4	91.6	90.8	90.6	89.7	90.0
7.400	53.8	61.1	62.4	54.3	62.3	90.0
10.990	0.0	65.0	104.1	111.3	128.4	90.0
13.130	0.0	67.3	81.6	125.8	127.5	90.0

**TABLE 8**  
**Grid Value  $\sigma$  for  $U_r^{10}$  (km/sec)**

U(km/sec)\ $\theta$	0.0	45.0	90.0
1.77	0.09	0.08	0.13
4.20	0.02	0.04	0.07
6.946	0.11	0.08	0.08
10.990	0.49	0.10	0.16
13.130	0.08	0.12	0.18



**TABLE 9**  
Grid Value  $\sigma$  for  $T_r$  (K)

U(km/sec)\ $\theta$	0.0	45.0	90.0
1.77	24	23	22
13.130	25	25	25

**TABLE 10**  
Grid Value  $\sigma$  for  $\theta$ , (deg)

U(km/sec)\ $\theta$	0.0	30.0	45.0	60.0	75.0	90.0
1.770	5.6	1.8	3.0	3.1	5.2	0.0
4.200	10.6	4.1	3.1	1.8	0.7	0.0
6.946	5.7	2.5	2.2	1.6	0.8	0.0
7.400	10.8	5.3	9.8	8.1	12.2	0.0
10.990	27.6	3.8	3.8	3.0	9.5	0.0
13.130	24.3	4.3	5.5	4.1	10.5	0.0

The full data set and residuals are given in Table 11. The residuals for the Knechtel and Pitts  $N_2^+$  data are also included, though they were not used in the least squares adjustment. It does not fit with this model. Table 12 provides the statistics for each data set separately.

**TABLE 11**  
**Residuals for Least Squares Fit**

Sp	U km/s	T K	Tw K	c	th	obs	res	$\sigma$	$\sigma'$	$\sigma''$	$\alpha$
N2	4.200	700	300	n	90	0.695	-0.003	0.646	0.698	1.363	0.879
N2	4.200	700	300	t	90	1.010	0.001	1.009	0.698	1.363	0.879
N2	4.200	700	300	n	80	0.689	-0.002	1.010	0.691	1.371	0.878
N2	4.200	700	300	t	80	1.010	0.000	1.010	0.691	1.371	0.878
N2	4.200	700	300	n	70	0.671	-0.001	1.010	0.672	1.391	0.877
N2	4.200	700	300	t	70	1.010	0.000	1.010	0.672	1.391	0.877
N2	4.200	700	300	n	60	0.643	0.004	1.010	0.639	1.426	0.876
N2	4.200	700	300	t	60	1.010	-0.000	1.010	0.639	1.426	0.876
N2	4.200	700	300	n	50	0.609	0.024	1.011	0.585	1.482	0.874
N2	4.200	700	300	t	50	1.010	-0.001	1.011	0.585	1.482	0.874
N2	4.200	700	300	n	40	0.572	0.021	1.010	0.551	1.524	0.896
N2	4.200	700	300	t	40	1.010	0.000	1.010	0.551	1.524	0.896
N2	4.200	700	300	n	30	0.538	-0.015	1.007	0.553	1.541	0.934
N2	4.200	700	300	t	30	1.010	0.003	1.007	0.553	1.541	0.934
N2	4.200	700	300	n	20	0.511	-0.026	1.011	0.537	1.590	0.964
N2	4.200	700	300	t	20	1.010	-0.001	1.011	0.537	1.590	0.964
N2	4.200	700	300	n	10	0.492	0.001	1.012	0.491	1.694	0.986
N2	4.200	700	300	t	10	1.010	-0.002	1.012	0.491	1.694	0.986
N2	4.200	700	300	n	0	0.486	0.030	1.008	0.456	1.843	1.000
N2	4.200	700	300	t	0	1.010	0.002	1.008	0.456	1.843	1.000
N2	7.420	700	300	b	90	0.160	-0.001	0.763	0.894	1.151	0.973
N2	7.420	700	300	b	75	0.130	-0.004	0.754	0.896	1.151	0.971
N2	7.420	700	300	b	60	0.100	0.010	0.829	0.887	1.165	0.969
N2	7.420	700	300	b	30	0.040	0.020	0.894	0.710	1.361	0.955
N2	7.420	700	300	b	15	-0.020	0.037	0.875	0.316	1.742	0.942
N2	7.420	700	300	b	90	0.195	0.034	0.763	0.894	1.151	0.973
N2	7.420	700	300	b	75	0.137	0.004	0.754	0.896	1.151	0.971
N2	7.420	700	300	b	60	0.080	-0.010	0.829	0.887	1.165	0.969
N2	7.420	700	300	b	45	0.070	0.000	0.898	0.836	1.223	0.966
N2	7.420	700	300	b	30	0.001	-0.019	0.894	0.710	1.361	0.955
N2	13.130	700	300	b	60	0.070	-0.140	1.204	0.851	1.177	0.961X
N2	13.130	700	300	b	30	0.030	-0.026	0.885	0.544	1.487	0.925X
N2	13.130	700	300	b	15	-0.040	0.163	0.717	0.307	1.726	0.884X
N2	13.130	700	300	b	90	0.100	-0.092	1.376	0.863	1.162	0.969X
N2	13.130	700	300	b	60	0.050	-0.160	1.204	0.851	1.177	0.961X
N2	13.130	700	300	b	45	0.020	-0.121	0.962	0.757	1.273	0.957X
N2	13.130	700	300	b	30	-0.010	-0.066	0.885	0.544	1.487	0.925X
N2	13.130	700	300	b	15	-0.130	0.073	0.717	0.307	1.726	0.884X
N2	13.130	700	300	n	90	0.857	-0.006	0.850	0.863	1.162	0.969
N2	13.130	700	300	n	90	0.886	0.023	0.850	0.863	1.162	0.969
N2	13.130	700	300	m	90	1.140	-0.022	0.850	0.863	1.162	0.969

**TABLE 11 (Continued)**  
**Residuals for Least Squares Fit**

Sp	U km/s	T K	Tw K	c	th	obs	res	$\sigma$	$\sigma'$	$\sigma''$	$\alpha$
N2	13.130	700	300	n	80	0.857	-0.010	1.385	0.867	1.158	0.966
N2	13.130	700	300	n	75	0.887	0.008	1.382	0.879	1.147	0.965
N2	13.130	700	300	m	75	1.140	-0.007	1.382	0.879	1.147	0.965
N2	13.130	700	300	n	70	0.857	-0.014	1.292	0.871	1.155	0.964
N2	13.130	700	300	n	60	0.824	-0.027	1.204	0.851	1.177	0.961
N2	13.130	700	300	n	60	0.838	-0.013	1.204	0.851	1.177	0.961
N2	13.130	700	300	m	60	1.190	0.013	1.204	0.851	1.177	0.961
N2	13.130	700	300	t	60	1.237	0.033	1.204	0.851	1.177	0.961
N2	13.130	700	300	n	50	0.764	-0.017	1.031	0.781	1.248	0.958
N2	13.130	700	300	t	50	1.000	-0.031	1.031	0.781	1.248	0.958
N2	13.130	700	300	n	45	0.792	0.035	0.962	0.757	1.273	0.957
N2	13.130	700	300	m	45	1.240	-0.033	0.962	0.757	1.273	0.957
N2	13.130	700	300	n	40	0.676	-0.025	0.938	0.701	1.330	0.947
N2	13.130	700	300	t	40	0.979	0.041	0.938	0.701	1.330	0.947
N2	13.130	700	300	n	30	0.538	-0.006	0.885	0.544	1.487	0.925
N2	13.130	700	300	n	30	0.551	0.007	0.885	0.544	1.487	0.925
N2	13.130	700	300	m	30	1.480	-0.007	0.885	0.544	1.487	0.925
N2	13.130	700	300	t	30	0.875	-0.010	0.885	0.544	1.487	0.925
N2	13.130	700	300	t	20	0.781	0.011	0.770	0.387	1.645	0.899
He	1.770	700	300	m	90	1.260	0.020	0.873	1.253	1.240	1.223
He	1.770	700	300	m	80	1.250	-0.009	0.747	1.226	1.259	1.220
He	1.770	700	300	t	80	0.740	-0.007	0.747	1.226	1.259	1.220
He	1.770	700	300	m	70	1.270	-0.014	0.718	1.204	1.284	1.215
He	1.770	700	300	t	70	0.730	0.012	0.718	1.204	1.284	1.215
He	1.770	700	300	m	60	1.300	-0.019	0.721	1.176	1.319	1.206
He	1.770	700	300	t	60	0.720	-0.001	0.721	1.176	1.319	1.206
He	1.770	700	300	m	50	1.380	0.013	0.727	1.135	1.367	1.194
He	1.770	700	300	t	50	0.720	-0.007	0.727	1.135	1.367	1.194
He	1.770	700	300	m	40	1.480	0.014	0.719	1.009	1.466	1.159
He	1.770	700	300	t	40	0.720	0.001	0.719	1.009	1.466	1.159
He	1.770	700	300	m	30	1.620	-0.015	0.717	0.739	1.635	1.084
He	1.770	700	300	t	30	0.720	0.003	0.717	0.739	1.635	1.084
He	1.770	700	300	m	20	1.840	0.002	0.701	0.361	1.838	0.982
He	1.770	700	300	t	20	0.700	-0.001	0.701	0.361	1.838	0.982
He	6.946	700	296	n	90	0.618	0.026	0.543	0.592	1.489	0.759
He	6.946	700	296	m	90	1.470	-0.019	0.543	0.592	1.489	0.759
He	6.946	700	296	n	75	0.574	-0.005	0.991	0.579	1.503	0.762
He	6.946	700	296	m	75	1.510	0.007	0.991	0.579	1.503	0.762
He	6.946	700	296	t	75	0.990	-0.001	0.991	0.579	1.503	0.762
He	6.946	700	296	n	60	0.514	-0.014	1.010	0.528	1.555	0.765
He	6.946	700	296	m	60	1.570	0.015	1.010	0.528	1.555	0.765
He	6.946	700	296	t	60	1.010	0.000	1.010	0.528	1.555	0.765

**TABLE 11 (Continued)**  
**Residuals for Least Squares Fit**

Sp	U km/s	T K	Tw K	c	th	obs	res	$\sigma$	$\sigma'$	$\sigma''$	$\alpha$
He	6.946	700	296	n	45	0.375	-0.040	1.009	0.415	1.664	0.767
He	6.946	700	296	m	45	1.700	0.036	1.009	0.415	1.664	0.767
He	6.946	700	296	t	45	1.010	0.001	1.009	0.415	1.664	0.767
He	6.946	700	296	m	30	1.800	-0.155	1.016	0.060	1.955	0.732
He	6.946	700	296	t	30	1.010	-0.006	1.016	0.060	1.955	0.732
He	6.946	700	296	m	15	2.620	0.049	1.00	-0.932	2.571	0.693
He	6.946	700	296	t	15	1.000	0.000	1.000	-0.932	2.571	0.693
Ar	10.990	700	300	n	90	0.896	-0.001	0.884	0.897	1.128	0.980
Ar	10.990	700	300	m	90	1.100	-0.028	0.884	0.897	1.128	0.980
Ar	10.990	700	300	n	90	0.926	0.029	0.884	0.897	1.128	0.980
Ar	10.990	700	300	n	80	0.863	-0.010	1.386	0.873	1.152	0.969
Ar	10.990	700	300	n	75	0.887	0.013	1.418	0.874	1.152	0.963
Ar	10.990	700	300	m	75	1.140	-0.012	1.418	0.874	1.152	0.963
Ar	10.990	700	300	n	70	0.813	-0.030	1.306	0.843	1.182	0.956
Ar	10.990	700	300	n	60	0.736	-0.032	1.169	0.768	1.257	0.940
Ar	10.990	700	300	n	60	0.745	-0.023	1.169	0.768	1.257	0.940
Ar	10.990	700	300	m	60	1.280	0.023	1.169	0.768	1.257	0.940
Ar	10.990	700	300	t	60	1.193	0.024	1.169	0.768	1.257	0.940
Ar	10.990	700	300	n	50	0.654	-0.026	1.120	0.680	1.345	0.920
Ar	10.990	700	300	t	50	1.111	-0.009	1.120	0.680	1.345	0.920
Ar	10.990	700	300	n	45	0.656	0.035	1.100	0.621	1.404	0.910
Ar	10.990	700	300	m	45	1.370	-0.034	1.100	0.621	1.404	0.910
Ar	10.990	700	300	n	40	0.577	0.006	1.007	0.571	1.454	0.911
Ar	10.990	700	300	t	40	0.996	-0.011	1.007	0.571	1.454	0.911
Ar	10.990	700	300	n	30	0.495	-0.010	0.862	0.505	1.524	0.913
Ar	10.990	700	300	n	30	0.509	0.004	0.862	0.505	1.524	0.913
Ar	10.990	700	300	m	30	1.520	-0.004	0.862	0.505	1.524	0.913
Ar	10.990	700	300	t	30	0.864	0.002	0.862	0.505	1.524	0.913
Ar	10.990	700	300	t	20	0.710	-0.073	0.783	0.459	1.579	0.915
N2+	8.300	700	300	n	90	0.902	0.059	0.819	0.843	1.195	0.957X
N2+	8.300	700	300	n	80	0.902	0.076	0.853	0.826	1.212	0.951X
N2+	8.300	700	300	n	75	0.896	0.080	0.846	0.816	1.222	0.948X
N2+	8.300	700	300	n	70	0.884	0.079	0.843	0.805	1.233	0.945X
N2+	8.300	700	300	n	60	0.854	0.074	0.832	0.780	1.261	0.937X
N2+	8.300	700	300	t	60	0.427	-0.405	0.832	0.780	1.261	0.937X
N2+	8.300	700	300	n	50	0.787	0.063	0.878	0.724	1.319	0.930X
N2+	8.300	700	300	t	50	0.506	-0.372	0.878	0.724	1.319	0.930X
N2+	8.300	700	300	n	40	0.701	0.051	0.879	0.650	1.395	0.922X
N2+	8.300	700	300	t	40	0.530	-0.349	0.879	0.650	1.395	0.922X
N2+	8.300	700	300	n	30	0.585	0.040	0.851	0.545	1.503	0.915X
N2+	8.300	700	300	t	30	0.494	-0.357	0.851	0.545	1.503	0.915X
N2+10.165		700	300	n	90	0.970	0.210	0.740	0.760	1.268	0.923X

**TABLE 11 (Continued)**  
**Residuals for Least Squares Fit**

Sp	U km/s	T K	Tw K	c	th	obs	res	$\sigma$	$\sigma'$	$\sigma''$	$\alpha$
N2+10.165		700	300	n	80	0.970	0.237	1.450	0.733	1.294	0.905X
N2+10.165		700	300	n	75	0.963	0.237	1.472	0.726	1.302	0.895X
N2+10.165		700	300	t	75	0.232	-1.240	1.472	0.726	1.302	0.895X
N2+10.165		700	300	n	70	0.963	0.272	1.298	0.691	1.336	0.885X
N2+10.165		700	300	t	70	0.378	-0.920	1.298	0.691	1.336	0.885X
N2+10.165		700	300	n	60	0.933	0.324	1.103	0.609	1.417	0.862X
N2+10.165		700	300	t	60	0.585	-0.518	1.103	0.609	1.417	0.862X
N2+10.165		700	300	n	50	0.896	0.387	1.061	0.509	1.515	0.838X
N2+10.165		700	300	t	50	0.677	-0.384	1.061	0.509	1.515	0.838X
N2+10.165		700	300	n	40	0.841	0.458	0.948	0.383	1.639	0.824X
N2+10.165		700	300	t	40	0.689	-0.259	0.948	0.383	1.639	0.824X
N2+10.165		700	300	n	30	0.738	0.461	0.794	0.277	1.743	0.824X
N2+10.165		700	300	t	30	0.683	-0.111	0.794	0.277	1.743	0.824X

In Table 11 the column labeled c indicates the observation type. An "n" denotes an observation of  $\sigma'$ , a "t" denotes an observation of  $\sigma$ , an "m" denotes an observation of  $\sigma''$ , and a "b" indicates an observation of the linear combination of  $\sigma$  and  $\sigma'$  given by Boring and Humphris. The calculated values of  $\sigma$ ,  $\sigma'$ ,  $\sigma''$ , and  $\alpha$  are also given. An "x" at the end of the line indicates that this observation was not used in the determination of the model parameters.

**TABLE 12**  
**Individual Statistics for Solution**

Specie	Velocity	<mean>	$\sigma$	Author
He	1.77	-0.001	0.012	Seidel and Steinheil
N <sub>2</sub>	4.1	0.000	0.008	Musanov and Nikiforov
He	6.69	-0.007	0.046	Liu, Sharma, and Knuth
N <sub>2</sub>	7.42	0.003	0.021	Boring and Humphris
Ar	10.99	-0.001	0.031	Doughty and Schaetzle
N <sub>2</sub>	13.13	-0.001	0.026	Doughty and Schaetzle
N <sub>2</sub>	13.13	-0.051	0.102	Boring and Humphris
All		-0.003	0.025	All

As an aid to viewing the scattering results, Figures 8, 9, and 10 show the two-dimensional dependence of  $U_s$ ,  $T_s$ , and  $\theta_s$  on  $U$  and  $\theta$ . The scattering angle surface reveals three regions. For intermediate  $6 > U > 3$  km/sec,  $\theta_s$  is between 60 and 90 deg, approaching a classical diffuse scattering regime. For lower velocities, it tends toward specular scattering. For higher velocities the scattering exhibits forward scattering where  $\theta_s > 90$  deg. Also for higher velocity, and  $\theta < 45$  deg, the scattering angle seems to follow  $\theta_s = 2\theta$ . The scattering velocity exhibits a different taxonomy. The scattering velocity, at grazing incidence  $\theta = 0$ , is well correlated but less than the incident velocity.

At  $\theta=90$  deg, the scattered velocity  $U$ , has a maximum at about  $U=4$  km/sec, a minimum at  $U=8$  km/sec, and a maximum again at  $U=11$  km/sec. At  $U=8$  km/sec the velocity is relatively constant, which is consistent with diffuse scattering.

231741-8

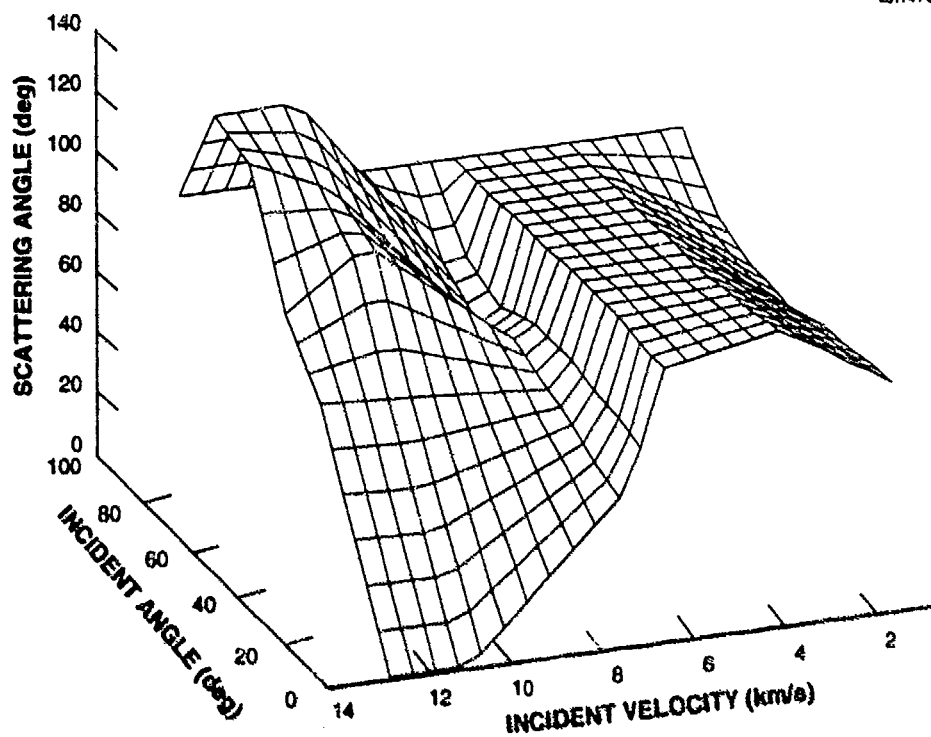


Figure 8. Scattering angle: helium on oxygen.

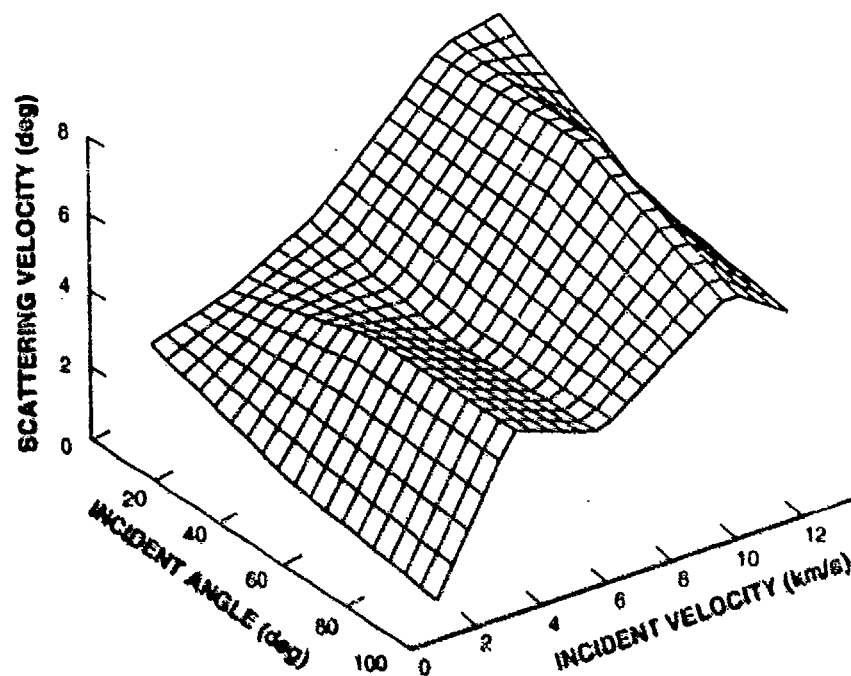


Figure 9. Scattering velocity: helium on oxygen.



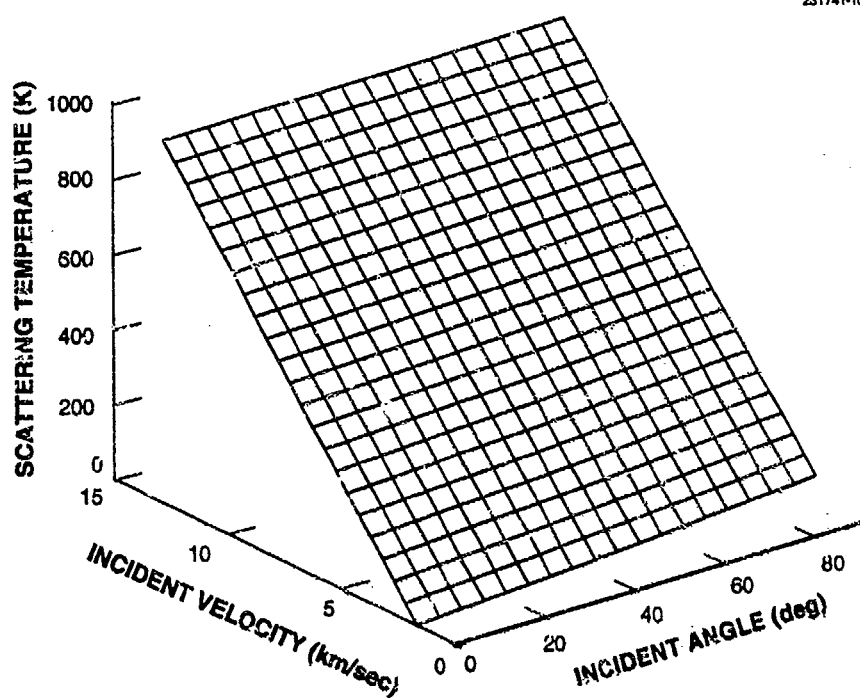


Figure 10. Scattering temperature: helium on oxygen.

## 8. CALCULATION OF $C_d$

### 8.1 COMPARISON OF GOODMAN AND WACHMAN THEORY AND HSN THEORY

The two formalisms for computing  $\alpha$  can hardly be expected to give the same result as they are based on quite different variables. The thermal accommodation coefficient of Goodman and Wachman (G&W) depends on the mass ratio ( $\mu=M/16$ ) in the temperature regime considered here. The HSN thermal accommodation coefficient depends primarily on the incident velocity  $U$  and secondarily on  $\mu$ ,  $T$ ,  $T_w$ , and  $\gamma$ . The HSN theory also includes the effects of a molecule's internal energy, which is assumed to be unchanged in the accommodating process. In addition, G&W give the range of validity for the theory as  $\mu < 0.83$ . In Figure 11 we plot  $\alpha$  derived from the two formulations. The HSN values are obtained with  $\theta=90^\circ$ . The figure uses the mass ratio  $\mu$  as the independent variable and plots the values of  $\alpha$ . The plotted points are in order of increasing  $\mu$ : H, He, N, O,  $N_2$ ,  $O_2$ , and Ar. The G&W values are consistently smaller than the HSN values. There is an observation of  $\alpha_0$  by Krech et al. [29]. They measured  $\alpha$  by scattering atomic oxygen off of three substances: RCG, nickel, and gold. It is argued that the atomic oxygen beam rapidly deposits an adsorbed layer of O atoms on the surface, and that the scattering surface is then effectively O; i.e.,  $\mu=1$ . Krech et al. give a value of  $\alpha=0.64\pm0.1$ , which is in close agreement with the value from the G&W theory.

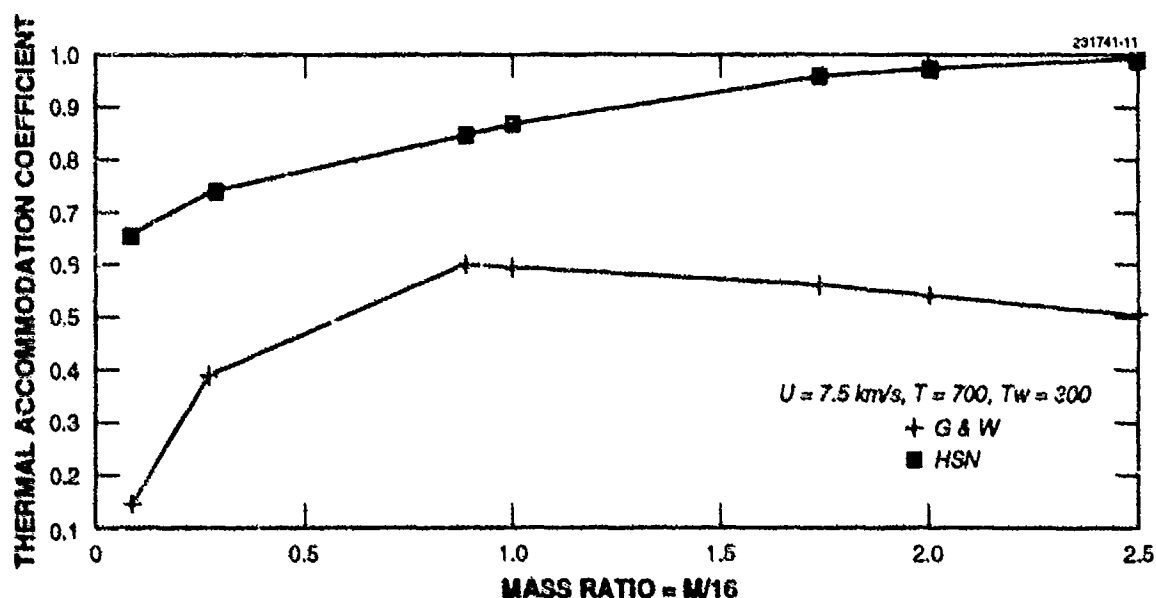


Figure 11. Comparison of G&W with HSN.

## 8.2 CALCULATION OF $C_d$ FOR FLAT PLATES

The HSN model obtained in Section 7 can now be used for calculation of  $C_d$ . First, examples are given for flat plates. In Figure 12 data are plotted as a function of  $\theta$  for  $N_2$  at an altitude of 200 km. The figure includes calculated values for  $\sigma=\text{sig}$ ,  $\sigma'=\text{sigp}$ , and  $\alpha=\text{alp}$ . Then, the Schaff and Chambre formulas are evaluated for  $C_d$  and  $C_l$ . Finally, the Schamberg formula for  $C_d'$  is shown. This last formula does not include any effects of the Maxwell thermal motion, though it uses the HSN derived value for  $\alpha$  consistent with  $\sigma$  and  $\sigma'$ . There is a large difference between the two models for  $C_d$ . Though it is not shown, the difference between the two models for  $C_l$  is similar.

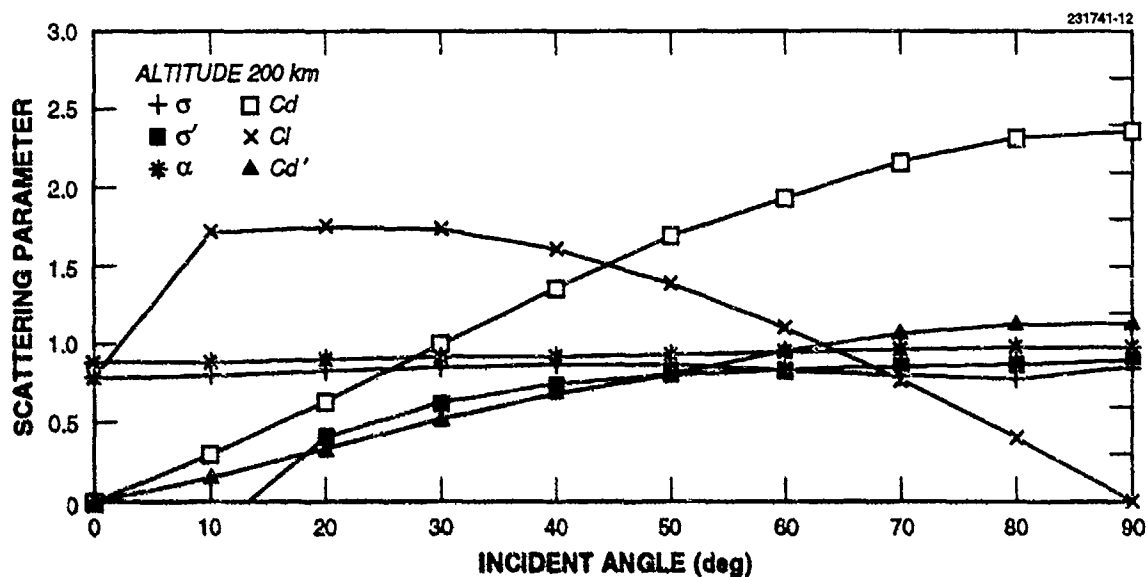


Figure 12. Flat plate  $C_d$  for  $N_2$

A second example is given for He at 800-km altitude in Figure 13. Again, the calculated accommodation coefficients and the resulting values for  $C_d$  and  $C_l$  are seen. In both cases, the difference between the Schaff and Chambre formulation and the Schamberg formulation is substantial, often exceeding a factor of two. In both cases, the Schaaf and Chambre formulation gives different results from the Schamberg approach.

## 8.3 $C_d$ FOR SPHERES

The calculation of  $C_d$  for spherical satellites can now be compared. In this case,  $C_d$  is calculated for each thermosphere constituent at a number of altitudes. It is calculated using the Schaaf and Chambre model  $C_d$ , the Schamberg model as modified by Alfonso et al.  $C_d'$ , and the Schamberg, Alfonso et al. model using the Goodman and Wachman formula for  $\alpha$   $C_d''$ .  $C_d'$  attempts to account for the thermal

motion of the Maxwell gas and the variation of  $\alpha$  with  $\theta$ , and  $C_d''$  only accounts for the thermal motion. Recall that the quadrature in  $\theta$  runs from  $-\pi/2$  to  $\pi/2$ . The HSN model evaluated for  $\theta < 0$  gives  $\sigma \approx \sigma' \approx \alpha \approx 0$ .

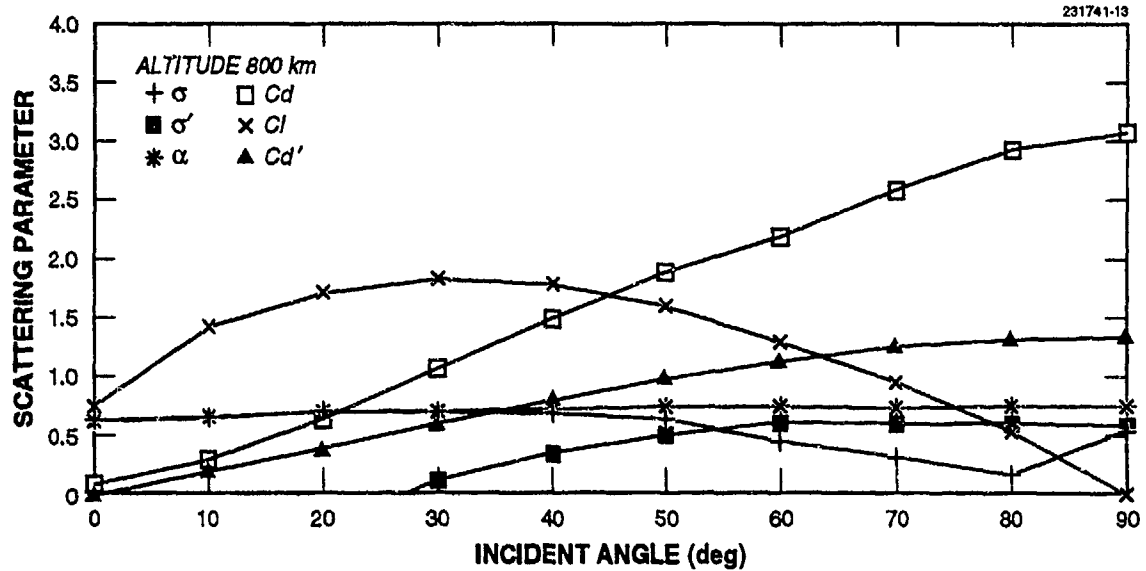


Figure 13. Flat plate  $C_d$  for helium.

There are important contributions to  $C_d$  for  $\theta < 0$ , especially when  $S=1$ . This is the case for the last example given; there, the thermal temperature is assumed to be 10000 K. This last case is the one studied by Alfonso et al., the Lageos satellite, that exhibits anomalous acceleration.

Table 13 gives the detailed results. In Figure 14,  $C_d$  is plotted as a function of velocity for some of the thermosphere constituents. In general the agreement between the Schaaf and Chambre model and the Schamberg, Alfonso et al. model is always less than  $\pm 10\%$ . However, the disagreement between the Schaaf and Chambre model and the Schamberg model with constant  $\alpha$  can be as much as 21%, and is generally greater than 10%. This is surprising given the much larger disagreement when the flat plate models are compared.

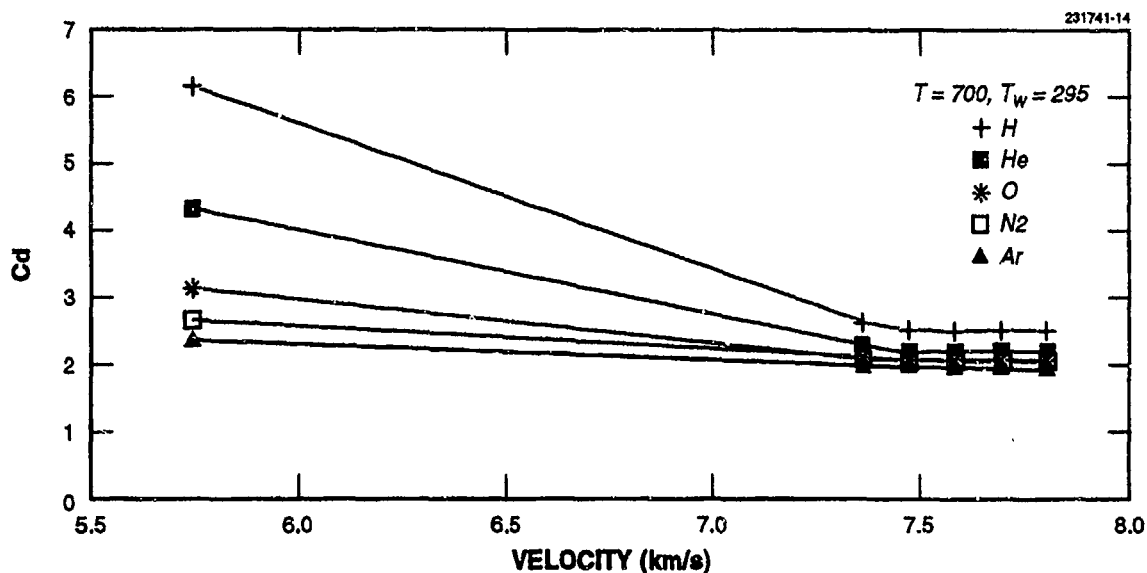


Figure 14.  $C_d$  for spherical satellites.

Now for altitudes less than 1000 km, the agreement of the three models for N and O is 2 to 3%. However, for all other constituents, the difference ranges from 11 to 19%. In particular, at 800 km, where He and O are the principal constituents, the errors are 17 and 4%, respectively.

For the case of a deep-space sphere, with high Maxwell temperature, the principal constituent is H. In this case, the error in  $C_d$  is +21%, i.e., one overestimates the drag force by 21%.

**TABLE 13**  
**C<sub>d</sub> for Spherical Satellites**

	q	V	T	T <sub>w</sub>	M	γ	C <sub>d</sub>	C <sub>d</sub> '	C <sub>d</sub> "	ε'	ε"
	km	km/s	K	K	amu						
H	200	7.784	700	295	1.008	1.667	2.7298	2.8629	3.1430	5	15
He	200	7.784	700	295	4.003	1.667	2.3960	2.5645	2.6608	7	11
N	200	7.784	700	295	14.004	1.667	2.2589	2.4033	2.3075	6	2
O	200	7.784	700	295	15.999	1.667	2.2403	2.3765	2.2993	6	3
N <sub>2</sub>	200	7.784	700	295	28.013	1.400	2.1265	2.2049	2.3741	4	12
O <sub>2</sub>	200	7.784	700	295	31.999	1.400	2.0913	2.1447	2.407	3	15
Ar	200	7.784	700	295	39.948	1.400	2.0773	2.0708	2.4654	-0	19
H	400	7.669	700	295	1.008	1.667	2.7271	2.8655	3.1534	5	16
He	400	7.669	700	295	4.003	1.667	2.3840	2.5610	2.6632	7	12
N	400	7.669	700	295	14.004	1.667	2.2459	2.3970	2.3082	7	3
O	400	7.669	700	295	15.999	1.667	2.2277	2.3698	2.2999	6	3
N <sub>2</sub>	400	7.669	700	295	28.013	1.400	2.1180	2.1963	2.3744	4	12
O <sub>2</sub>	400	7.669	700	295	31.999	1.400	2.0859	2.1362	2.4074	2	15
Ar	400	7.669	700	295	39.948	1.400	2.0796	2.0705	2.465	-0	19
H	600	7.558	700	295	1.008	1.667	2.7252	2.8681	3.1637	5	16
He	600	7.558	700	295	4.003	1.667	2.3727	2.5576	2.6657	8	12
N	600	7.558	700	295	14.004	1.667	2.2337	2.3908	2.3088	7	3
O	600	7.558	700	295	15.999	1.667	2.2159	2.3632	2.3004	7	4
N <sub>2</sub>	600	7.558	700	295	28.013	1.400	2.1105	2.1879	2.3748	4	13
O	600	7.558	700	295	31.999	1.400	2.0817	2.1282	2.4077	2	16
Ar	600	7.558	700	295	39.948	1.400	2.0810	2.0704	2.4658	-1	18
H	800	7.452	700	295	1.008	1.667	2.7240	2.8707	3.1741	5	17
He	800	7.452	700	295	4.003	1.667	2.3621	2.5543	2.6682	8	13
N	800	7.452	700	295	14.004	1.667	2.2222	2.3847	2.3094	7	4
O	800	7.452	700	295	15.999	1.667	2.2048	2.3568	2.3010	7	4
N <sub>2</sub>	800	7.452	700	295	28.013	1.400	2.1039	2.1797	2.3751	4	13
O <sub>2</sub>	800	7.452	700	295	31.999	1.400	2.0788	2.1205	2.4080	2	16
Ar	800	7.452	700	295	39.948	1.400	2.0819	2.0702	2.4661	-1	18
H	1000	7.350	700	295	1.008	1.667	2.7820	2.8738	3.1844	3	14
He	1000	7.350	700	295	4.003	1.667	2.4102	2.5511	2.6707	6	11
N	1000	7.350	700	295	14.004	1.667	2.2574	2.3787	2.3101	5	2
O	1000	7.350	700	295	15.999	1.667	2.2371	2.3504	2.3015	5	3
N <sub>2</sub>	1000	7.350	700	295	28.013	1.400	2.1164	2.1717	2.3754	3	12
O <sub>2</sub>	1000	7.350	700	295	31.999	1.400	2.0858	2.1134	2.4083	1	15
Ar	1000	7.350	700	295	39.948	1.400	2.0826	2.0700	2.4663	-1	18
H	5800	5.721	10000	295	1.008	1.667	6.1588	5.8562	7.4522	-5	21
He	5800	5.721	10000	295	4.003	1.667	4.2973	3.9866	4.4837	-7	4
N	5800	5.721	10000	295	14.004	1.667	3.1747	2.8608	2.8196	-10	-11
O	5800	5.721	10000	295	15.999	1.667	3.0663	2.7774	2.7487	-9	-10
N <sub>2</sub>	5800	5.721	10000	295	28.013	1.400	2.5311	2.3946	2.6439	-5	4
O <sub>2</sub>	5800	5.721	10000	295	31.999	1.400	2.3808	2.2974	2.6473	-4	11
Ar	5800	5.721	10000	295	39.948	1.400	2.2660	2.2118	2.6632	-2	18

C<sub>d</sub> using Schaaf and Chambre formulas with variable σ(θ) and σ'(θ).

C<sub>d</sub>' using Schamberg, Alfonso et al. with variable α(θ).

C<sub>d</sub>" using Schamberg, Alfonso et al. with constant α from Goodman and Wachman.

ε' = 100(C<sub>d</sub>' - C<sub>d</sub>)/C<sub>d</sub>

ε" = 100(C<sub>d</sub>" - C<sub>d</sub>)/C<sub>d</sub>

Figures 15 through 21 present the dependence of  $C_d^{Sp}$  for each thermosphere constituent as a function of velocity for a number of temperatures. Figures 22 through 28 present the dependence of  $C_d^{Sp}$  for each thermosphere constituent as a function of temperature for a number of velocities.

#### 8.4 COMPARISON OF $C_d$ WITH HERRERO

Herrero [30,31] tried to calculate the effective  $C_d$  for a cylindrical spacecraft with motion along the axis of symmetry. He showed that the contribution to  $C_d$  of the lateral surface, parallel to the motion, is  $2(L/r)C_{LS}$ , where  $L$  is the length of the cylinder,  $r$  is the radius of the cylinder, and  $C_{LS}$  is the drag coefficient for the surface element. Though a novel approach, he estimated that  $0.07 < C_{LS} < 0.06$ . The theory here gives, for  $N_2$  at 200-km altitude,  $C_{LS}=0.0378$ . If we adopt Herrero's estimate for the contribution of the nose cone as  $C_{Df}=1.5$ , and  $L/r=10$ , we obtain

$$C_d = C_{Df} + 2 \frac{L}{r} C_{LS} = 1.5 + 0.76 = 2.26$$

Herrero's estimate ranged between 2.7 and 2.9.

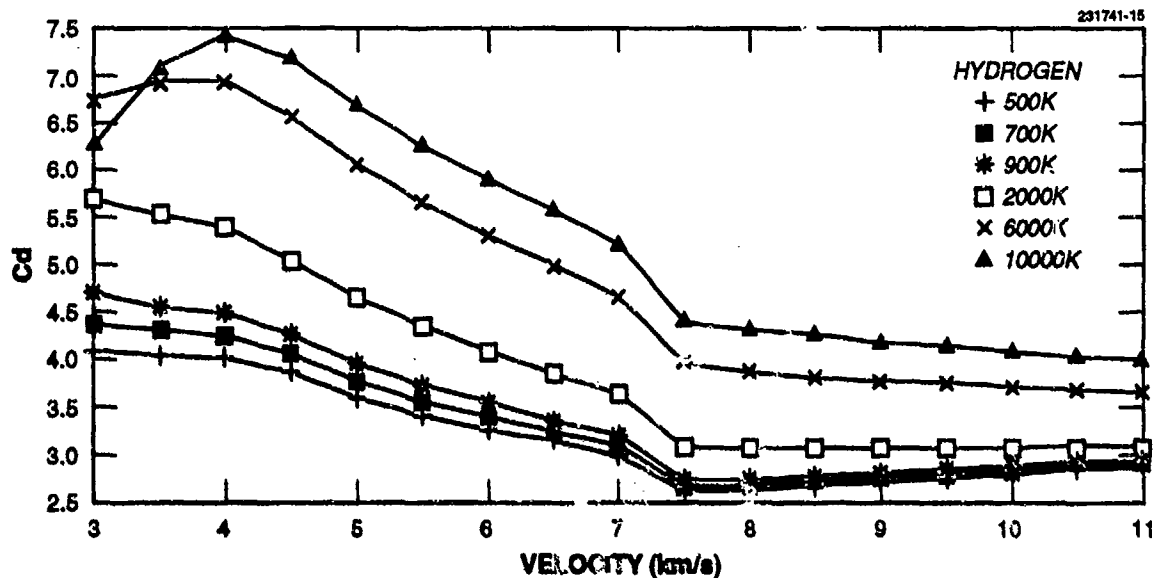


Figure 15.  $C_d$  for sphere: hydrogen.

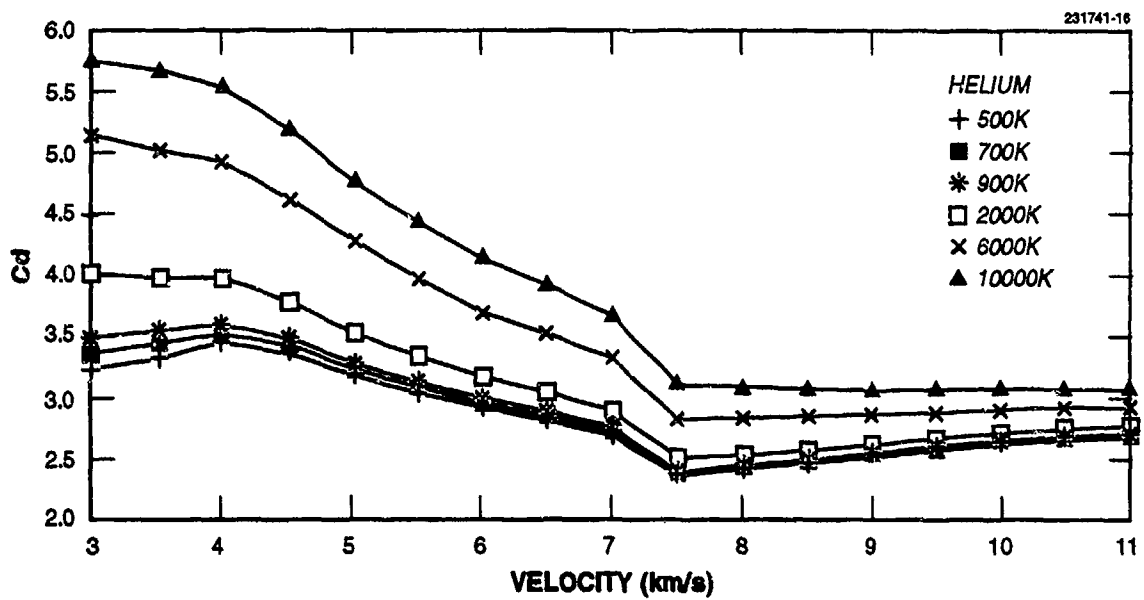


Figure 16.  $C_d$  for sphere: helium.

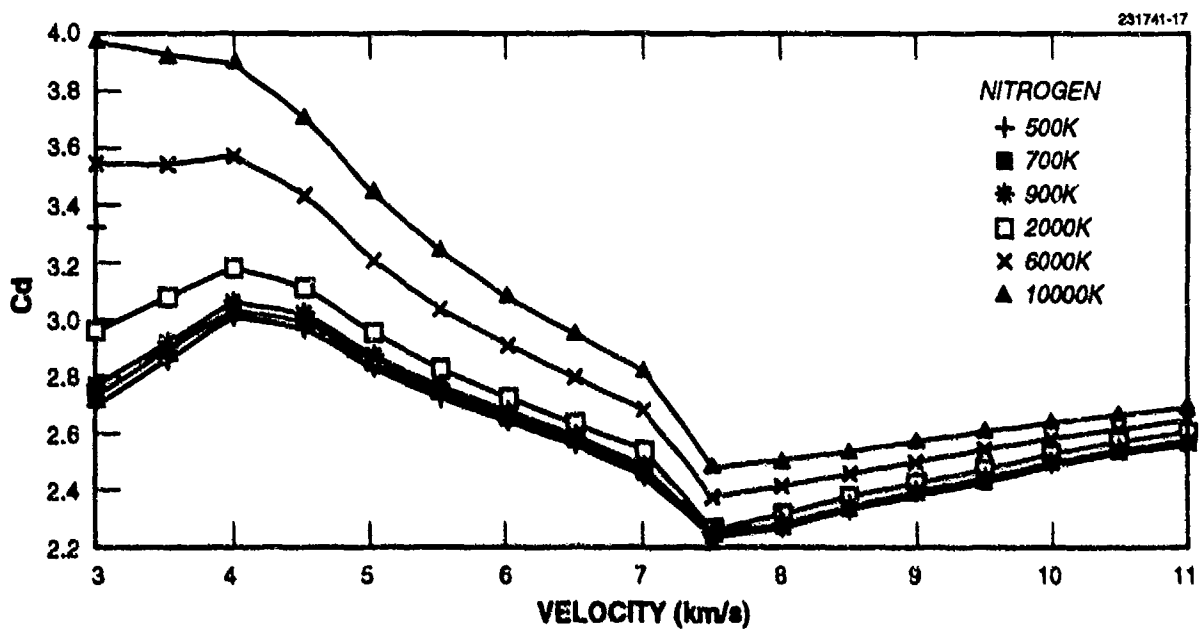


Figure 17.  $C_d$  for sphere: nitrogen.



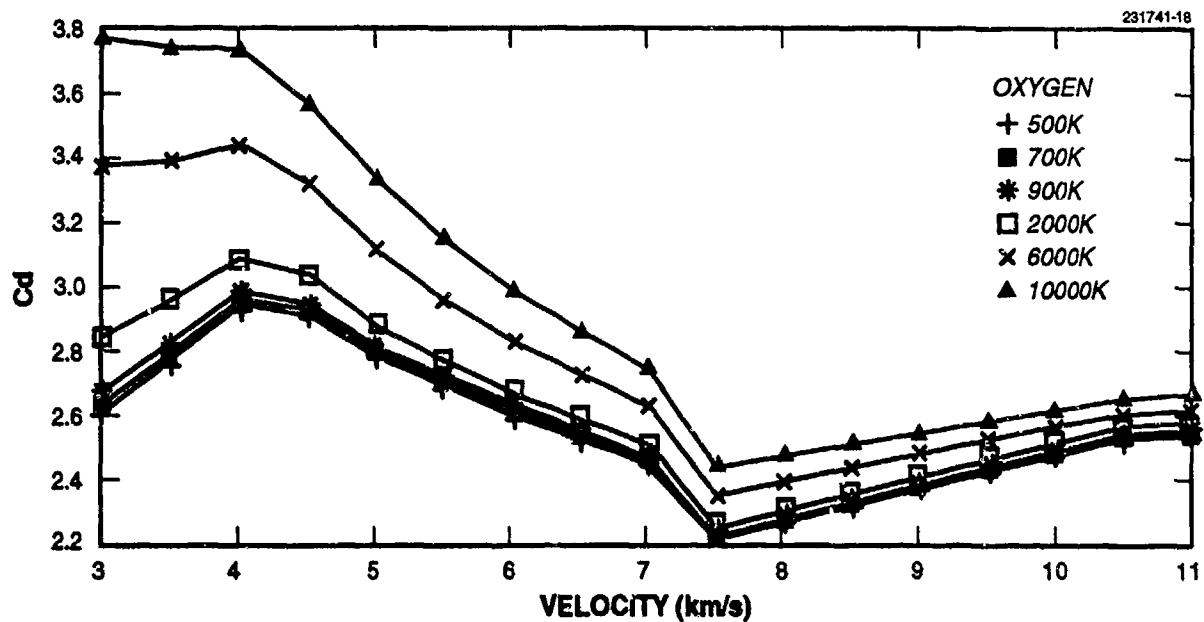


Figure 18.  $C_d$  for sphere: oxygen.

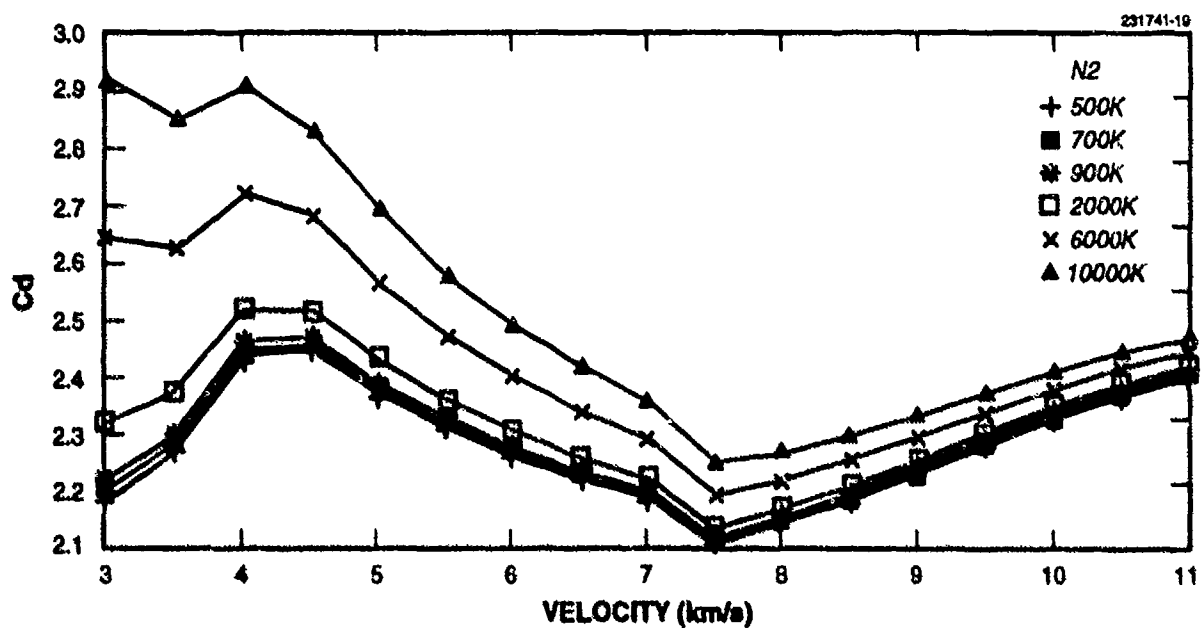


Figure 19.  $C_d$  for sphere:  $N_2$ .

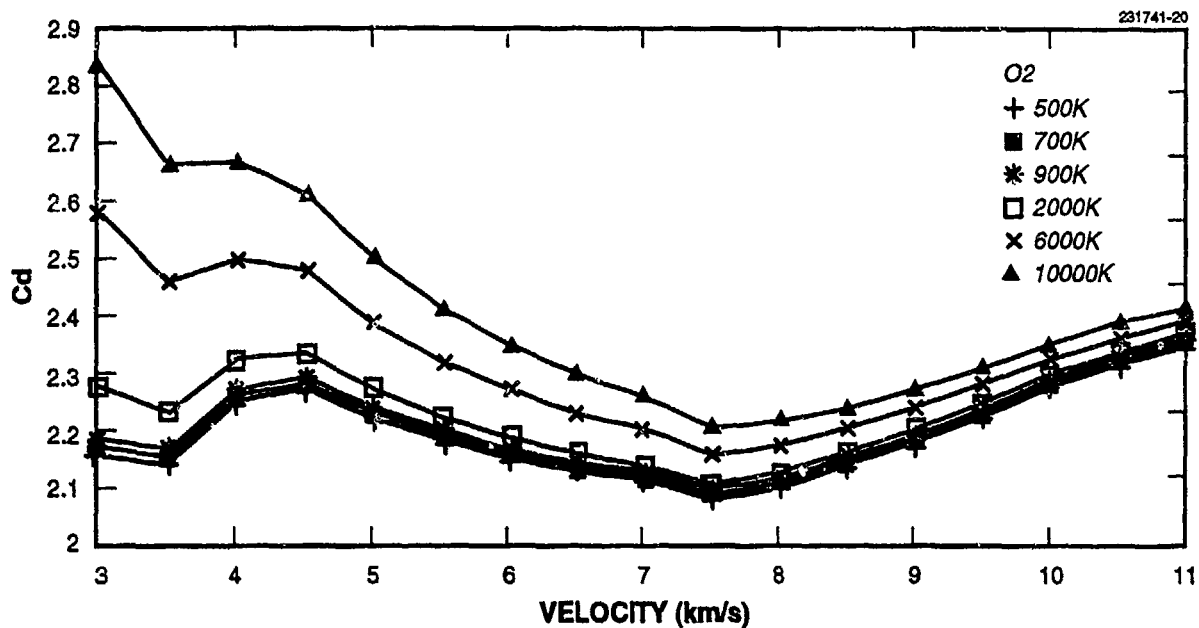


Figure 20.  $C_d$  for sphere: O<sub>2</sub>

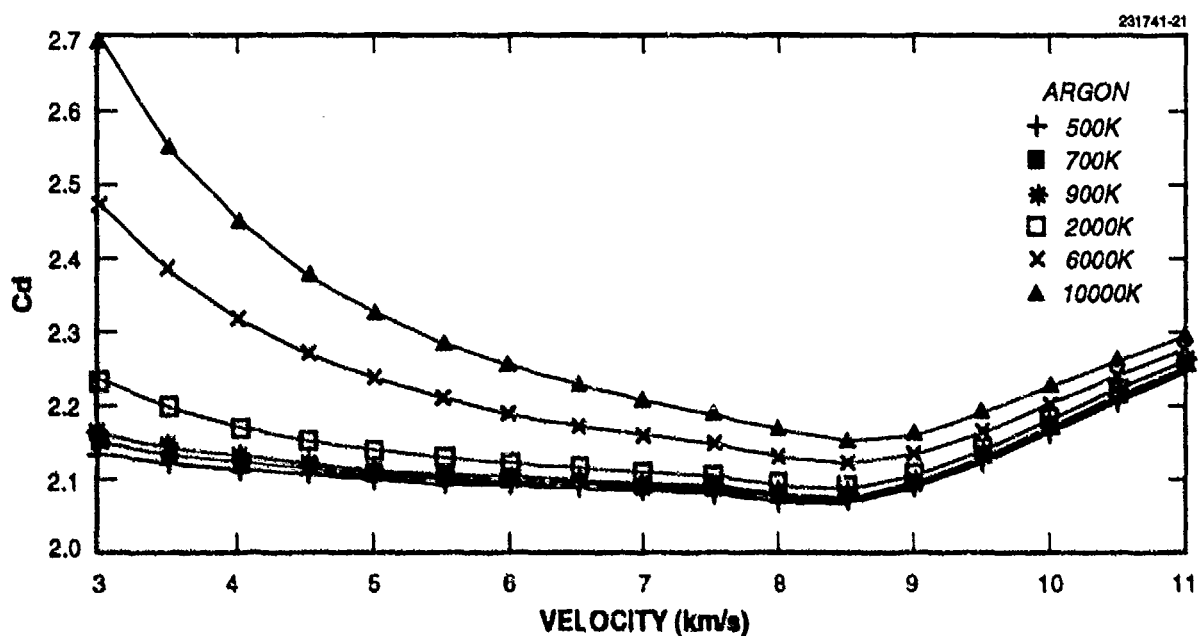


Figure 21.  $C_d$  for sphere: argon.

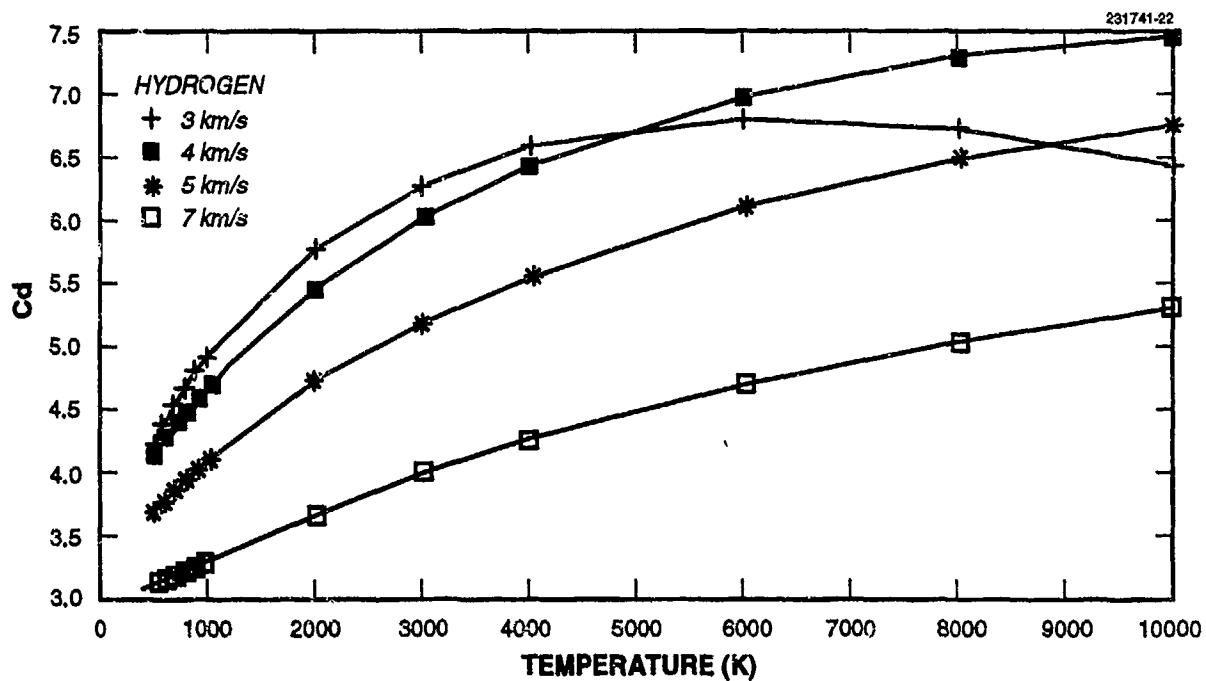


Figure 22.  $C_d$  for sphere: hydrogen.

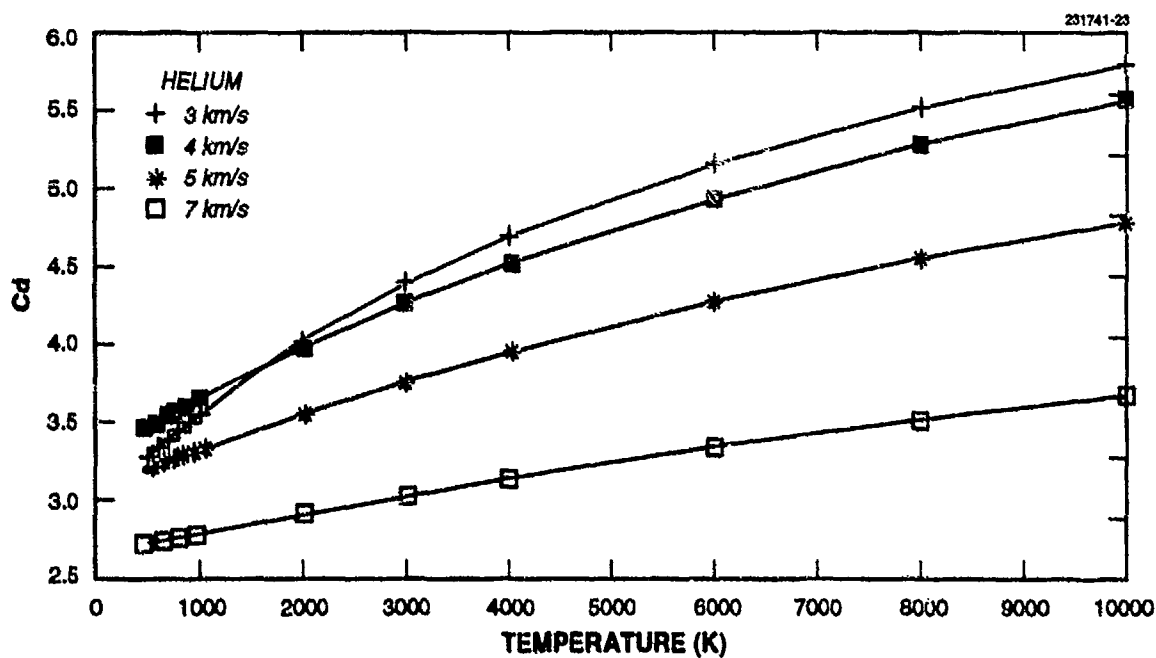


Figure 23.  $C_d$  for sphere: helium.

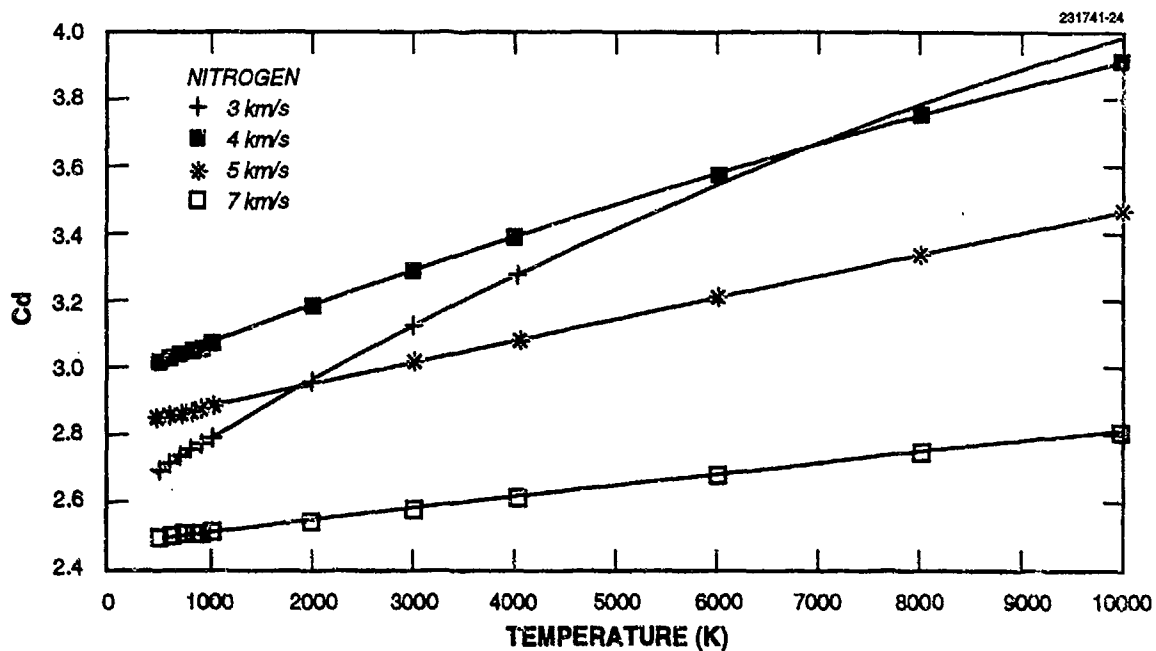


Figure 24.  $C_d$  for sphere: nitrogen.

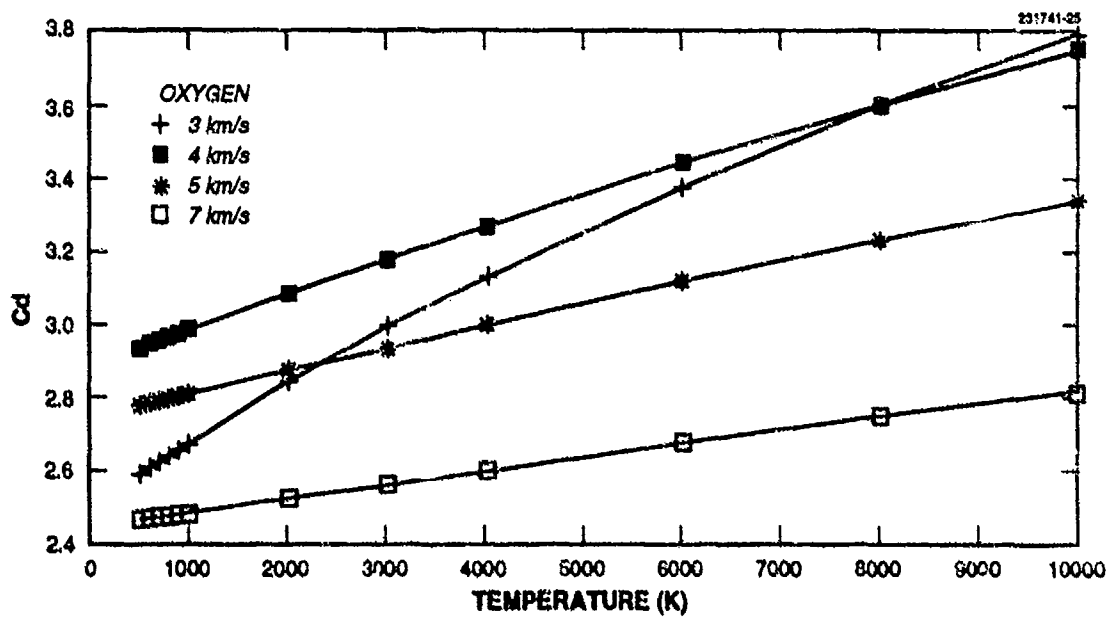


Figure 25.  $C_d$  for sphere: oxygen.

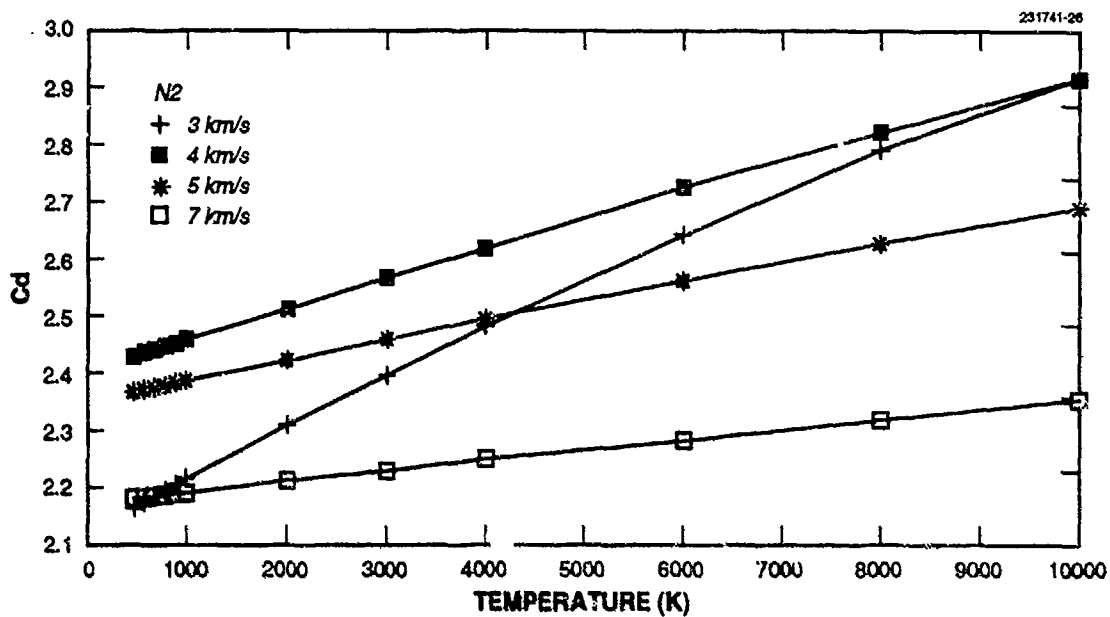


Figure 26.  $C_d$  for sphere:  $N_2$

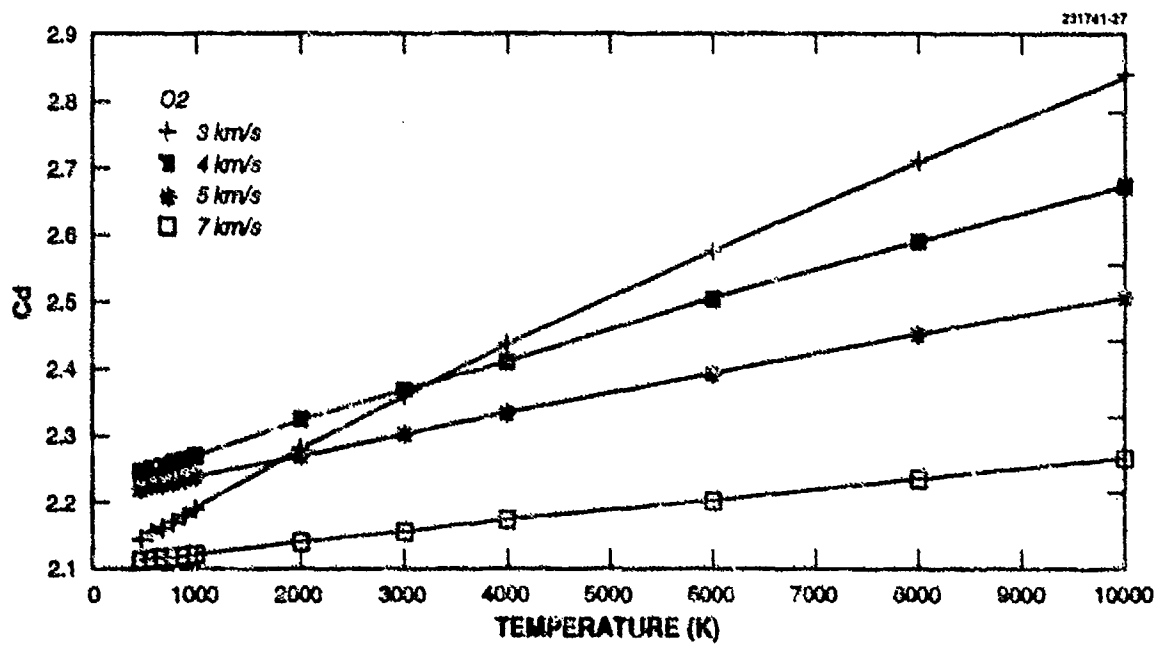


Figure 27.  $C_d$  for sphere:  $O_2$

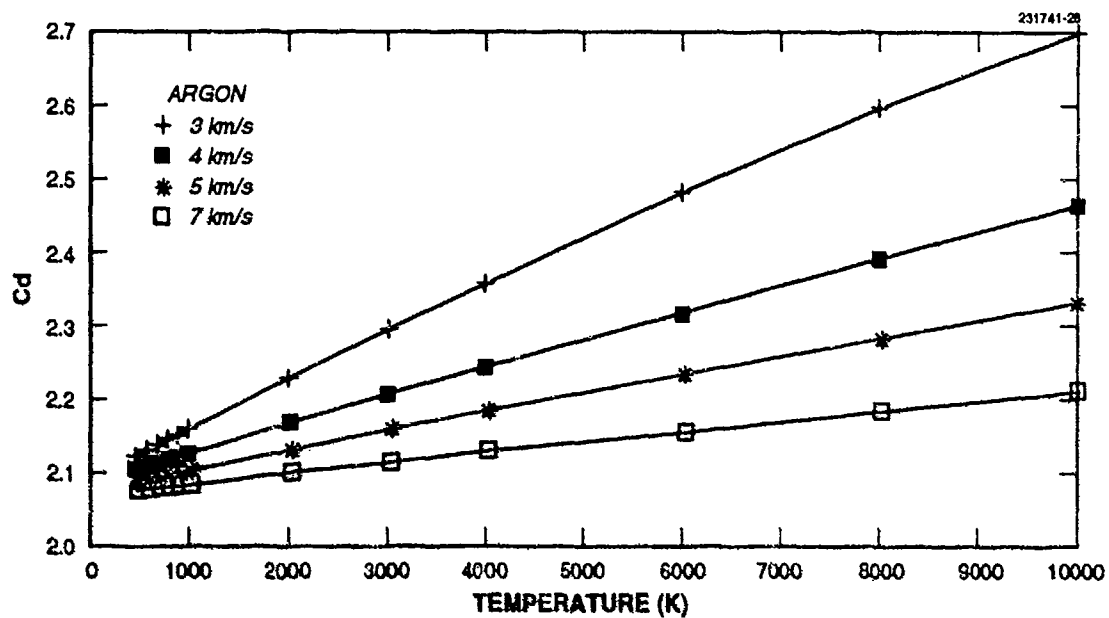


Figure 28.  $C_d$  for sphere: argon.

## 9. SUMMARY

We have developed a model for scattering that is appropriate for satellite conditions, i.e., satellite velocities and materials and thermosphere constituents and temperatures. The model is based on the formalism of Hurlbut, Sherman, and Nocilla (the HSN model) and uses published data on momentum accommodation coefficients to determine the underlying parameters. The model agrees with observed momentum accommodation coefficients to 2.5%. Though applied to the seven atmospheric constituents, the model is limited to velocities between 1.77 and 13.66 km/sec and to scattering surfaces that can reasonably be viewed as presenting oxygen atoms to the impinging particles.

The HSN model predicts the three accommodation coefficients,  $\sigma$ ,  $\sigma'$ , and  $\alpha$ , as a function of incident angle. This allows a comparison of the ballistic coefficient model of Schaaf and Chambre [15] (based on  $\sigma$  and  $\sigma'$ ) and that of Schamberg [10,11] (based on  $\alpha$ ). Schamberg's model is the basis of many aeronomy analyses [4]. Schamberg's model does not account for the thermal motion of the impinging molecules and assumes the scattered molecules are fully accommodated and scattered diffusely. Alfonso et al. [16] tried to extend Schamberg's model to account for atmospheric thermal motion for spherical satellites. We have been unable to fully reconcile these two approaches. The Schaaf and Chambre approach is adopted as more fundamental, making fewer assumptions.

The agreement of the Schaaf and Chambre model and the Schamberg model, using the HSN theory to determine scattering properties, is no better than a factor of two. When applied to spheres, taking into account the aspect dependence of  $\alpha$ , the two models agree to better than 10%. However, using a constant  $\alpha$ , the Schamberg, Alfonso et al. model has errors exceeding 20%.

For application of these models to calculation of satellite drag, one can expect an error exceeding 20%, using the simple ballistic coefficient. The errors are not constant, depending on altitude and thermosphere constituent. Therefore, one can expect a significant contribution to the calculation of satellite drag from unmodeled errors in accommodation coefficients and ballistic coefficients, even for spherical satellites.

## REFERENCES

1. E.M. Gaposchkin and A.J. Coster, "Analysis of satellite drag," *Lincoln Lab. J.* **1**, 203-224 (1988).
2. F.A. Marcos, "Accuracy of atmospheric drag models at low satellite altitudes," *Adv. Space Res.* **10**, (3)417-(3)422 (1990).
3. F.A. Marcos, C.R. Baker, J.N. Bass, T.L. Killeen, and R.G. Roble, "Satellite Drag Models; Current Status and Prospects," presented at AAS/AIAA Astrodynamics Specialist Conference, Victoria, B.C., Canada, August 16-19, 1993.
4. G.E. Cook, "Satellite drag coefficients," *Planet. Space Sci.* **13**, 929-946 (1965).
5. A.H. Hedin, "A revised thermospheric model based on mass spectrometer and incoherent scatter data: MSIS 83," *J. Geophys. Res.* **A88**, 170 (1983).
6. M. Seidl and E. Steinheil, "Measurements of momentum accommodation coefficients on surfaces characterized by Auger spectroscopy, SIMS and LEED," in M. Becker and M. Fiebig (eds) *Rarefied Gas Dynamics*, Vol 2, DFVLR-Press, Porz-Wahn, Paper E.9, (1974) E.9-1-E.9012.
7. S.M. Liu, P.K. Sharma, and E.L. Knuth, "Satellite drag coefficients calculated from measured distributions of reflected helium atoms," *AIAA J.* **17**, 1314-1319 (1979).
8. F.C. Hurlbut, "Particle surface interaction in the orbital context: A survey," *Prog. Astronaut. Astrodynam.* **116** 419-450 (1989).
9. E.L. Knuth, "Free molecule normal-momentum transfer at satellite surfaces," *AIAA J.* **18**, 602-605 (1980).
10. R. Schamberg, "A new analytic representation of surface interaction for hyperthermal free molecule flow with application to neutral-particle drag estimates of satellites," Project Rand Research Memorandum RM-2313, (ASTIA Document No. AD 215301) The Rand Corporation, Santa Monica, California, January 8, (1959).
11. R. Schamberg, "A new analytic representation of surface interaction for hyperthermal free-molecule flow with application to satellite drag," *Proceedings of 1959 Heat Transfer and Fluid Mech Inst*, Palo Alto: Stanford Univ. Press, (1959).
12. F.C. Hurlbut, "Gas/surface scatter models for satellite applications", *Prog. Astronaut. Aeronaut.* **103**, 97-119 (1986).
13. G.E. Cook, "Drag coefficients of spherical satellites," *Ann. Geophys.* **22**, 53-64 (1966).
14. S.A. Schaaf, "Mechanics of rarefied gasses," in S. Flugge (ed) *Handbuch der Physik*, Vol VIII/2, Berlin: Springer Verlag, (1963), 591-624.



## REFERENCES (Continued)

15. S.A. Schaaf and P.L. Chambre, "Flow of rarefied gases," in H.W. Emmons (ed) *High Speed Aerodynamics and Jet Propulsion*, Vol III, Sect H, Princeton Aeronautical Paperbacks, (1961), 687-736.
16. G. Alfonso, F. Barlier, C. Berger, F. Mignard, and J.J. Walch, "Reassessment of the charge and neutral drag of Lageos and its geophysical implications," *J. Geophys. Res.* **90**, 9381-9398 (1985).
17. F.C. Hurlbut, "Two contrasting modes for description of wall/gas interactions," *Prog. Astronaut. Astrodynam.* (1993).
18. P.M. Morse, *Thermal Physics*, New York: W.A.Bengamin, Inc., (1965).
19. F.C. Hurlbut and F.S. Sherman, "Application of the Nocilla wall reflection model to free-molecule kinetic theory," *Phys. Fluids*, **11**, 486-496 (1968).
20. B. Baule, *Phys.* **44**, 45 (1914).
21. F.O. Goodman and H.Y. Wachman, "Formula for thermal accommodation coefficients," *J. Chem. Phys.* **46**, 2376-2386 (1967).
22. S.V. Musanov, A.P. Nikiforov, A.I. Omelik, and O.G. Freedlander, "Experimental Determination of Momentum Transfer Coefficients in Hypersonic Free Molecular Flow and Distribution Function Recovery of Reflected Molecules", in O.M. Belotserkovskii, M.N. Kogan, S.S. Kutatedladze, and A.R. Rebrov (eds.) *Proc. 13th International Symp.on Rarefied Gas Dynamics*, New York: Plenum Press, Vol 1, (1985), 669-676.
23. J.W. Boring and R.R. Humphris, "Drag coefficients for free molecule flow in the velocity range 7-37 mk/sec," *AIAA J.* **8** 1658-1662 (1970).
24. R.O. Doughty and W.J. Schaeztle, "Experimental determination of momentum accommodation coefficients at velocities up to and exceeding earth escape velocity," in L. Trilling and H.Y. Wachman (eds.) *Rarefied Gas Dynamics*, New York: Academic Press (1969) Vol. 2, 1035-1054.
25. W.J. Schaeztle, "Some experimental data on momentum accommodation coefficients," in C.L. Brundin (ed) *Rarefied Gas Dynamics*, Vol 1, New York: Academic Press (1967), 211-222.
26. E.D. Knechtel and W.C. Pitts, "Experimental momentum accommodation on metal surfaces of ions near and above earth satellite speed," in L. Trilling and H.Y. Wachman (eds.) *Rarefied Gas Dynamics*, New York: Academic Press (1969), Vol. 2, 1257-1266.
27. E.D. Knechtel and W.C. Pitts, "Normal and tangential momentum accommodation for earth satellite conditions," *Astronautica Acta* **18**, 171-184 (1973).

## REFERENCES (Continued)

28. Biermann, "Factorization Methods for Discrete Sequential Estimation," New York: Academic Press (1977).
29. R.H. Krech, M.J. Gauthier, and G.E. Caledonia, "High velocity atomic oxygen/surface accommodation studies," *J. Spacecr. Rockets* 30, 509-513 (1993).
30. F.A. Herrero, "The drag coefficient of cylindrical spacecraft in orbit at altitudes greater than 150km," NASA Technical Memorandum 85043, Goddard Space Flight Center, Greenbelt, MD, May 1983.
31. F.A. Herrero, "The lateral surface drag coefficient of cylindrical spacecraft in a rarefied finite temperature atmosphere," *AIAA J.* 23, 862-867 (1985).

# REPORT DOCUMENTATION PAGE

Form Approved  
OMB No. 0704-0188

Public reporting burden for this collection of information is estimated to average 1 hour per response, including the time for reviewing instructions, searching existing data sources, gathering and maintaining the data needed, and completing and reviewing the collection of information. Send comments regarding this burden estimate or any other aspect of this collection of information, including suggestions for reducing this burden, to Washington Headquarters Services, Directorate for Information Operations and Reports, 1215 Jefferson Davis Highway, Suite 1204, Arlington, VA 22202-4302, and to the Office of Management and Budget, Paperwork Reduction Project (0704-0188), Washington, DC 20503.

1. AGENCY USE ONLY (Leave blank)		2. REPORT DATE 18 July 1994		3. REPORT TYPE AND DATES COVERED Technical Report	
4. TITLE AND SUBTITLE  Calculation of Satellite Drag Coefficients				5. FUNDING NUMBERS  C — F19628-90-C-0002 PR — 311	
6. AUTHOR(S)  Edward M. Gaposchkin					
7. PERFORMING ORGANIZATION NAME(S) AND ADDRESS(ES)  Lincoln Laboratory, MIT P.O. Box 73 Lexington, MA 02173-9108				8. PERFORMING ORGANIZATION REPORT NUMBER  TR-998	
9. SPONSORING/MONITORING AGENCY NAME(S) AND ADDRESS(ES)  Space Missile Center P.O. Box 92960 Los Angeles AFB, Los Angeles CA 90009				10. SPONSORING/MONITORING AGENCY REPORT NUMBER  ESC-TR-93-293	
11. SUPPLEMENTARY NOTES  None					
12a. DISTRIBUTION/AVAILABILITY STATEMENT  Approved for public release; distribution is unlimited.				12b. DISTRIBUTION CODE	
13. ABSTRACT (Maximum 200 words)  Calculation of $C_d$ for satellites using accommodation coefficients is reviewed. A phenomenological model for accommodation coefficients due to Hurlbut, Sherman, and Nocilla is used to obtain values for the accommodation coefficients for average satellite materials, thermosphere constituents and temperatures, and satellite velocities using a number of laboratory measurements. There is a significant difference between these results and the traditional method of calculating $C_d$ . These differences contribute as much as 20% error in use of thermosphere models for calculation of satellite drag.					
14. SUBJECT TERMS thermosphere drag coefficients accommodation coefficients  atmospheric drag ballistic coefficients				15. NUMBER OF PAGES 72	
				16. PRICE CODE	
17. SECURITY CLASSIFICATION OF REPORT Unclassified	18. SECURITY CLASSIFICATION OF THIS PAGE Unclassified	19. SECURITY CLASSIFICATION OF ABSTRACT Unclassified	20. LIMITATION OF ABSTRACT Same as Report		

NSN 7540-01-280-5500

Standard Form 298 (Rev. 2-89)  
Prescribed by ANSI Std. Z39-18  
298-102